Parameter-Free Prediction of DNA Conformations in Elongational Flow by Successive Fine Graining

P. Sunthar and J. Ravi Prakash*

Department of Chemical Engineering, Monash University, Melbourne, VIC 3800, Australia
Received December 18, 2003; Revised Manuscript Received October 21, 2004

ABSTRACT: Brownian dynamics simulations are used to predict the evolution of DNA conformations in elongational flow. The DNA molecule is represented by a bead−spring chain model, and excluded-volume and hydrodynamic interactions between the beads are taken into account. Two distinct types of behavior are examined, corresponding to infinite and finite chains. In the former case, Hookean springs are used, and simulations data accumulated for chains with increasing numbers of beads, N, are extrapolated to the limit $N \rightarrow \infty$. In this nondraining limit, universal DNA stretch vs strain curves are obtained as a function of the solvent quality parameter z. In the case of finite chains with N_k Kuhn steps, finitely extensible springs are used, and the extrapolation of finite chain data is restricted to the limit $(N - 1) \rightarrow N_k$. It is shown that in the presence of finitely extensible springs both the excluded-volume and hydrodynamic interaction parameters need to be redefined appropriately. The role of finite size effects and sensitivity to the choice of parameter values is examined by comparing the finite chain stretch vs strain curves with the universal curves. Theoretical predictions are also shown to compare favorably with experimental observations of DNA stretch.

1. Introduction

The measurement and prediction of the properties of dilute polymer solutions, both at equilibrium and in the presence of an induced flow, has been a fundamental concern of polymer physics. Until relatively recently, the validation of statistical theories of polymer solution dynamics has largely been confined to comparing predictions of macroscopic observables, such as viscoelastic properties, with experimental observations. However, recent experiments on dilute solutions of DNA molecules,[1−4] in which a protocol for the measurement of certain microscopic quantities was introduced, have raised the issue of theoretical validation to a new level. Smith and Chu[3] observed, under a microscope, the evolution of λ-phage DNA molecules in an elongational field in a tiny cross slot cell and measured the total extent of the molecules, as they were stretched from a coillike state to the fully elongated state. As a result, they were able to obtain one of the first direct measurements of a microscopic quantity that is characteristic of a dilute polymer solution undergoing flow. While recent advances in the theoretical description of polymer solution dynamics have shown that it is essential to take into account the existence of certain nonlinear microscopic phenomena (which are neglected in the Rouse theory[5,6]), to obtain accurate predictions of macroscopic variables, the experimental results of Chu and coworkers provide an opportunity, for the first time, to examine the importance of these phenomena in the context of microscopic variables.

The most important development in molecular theories for the equilibrium and linear viscoelastic behavior of dilute polymer solutions, since the introduction of the Rouse theory (which represents the polymer molecule by a chain of N beads connected together by $(N - 1)$ linear Hookean springs), has been the recognition that the incorporation of excluded-volume (EV) effects is necessary in order to explain the scaling behavior of static properties (such as the radius of gyration) in good solvents, while the incorporation of hydrodynamic interactions (HI) is required to explain the scaling of dynamic properties (such as the diffusivity and intrinsic viscosity). In addition, far from equilibrium, it has been found necessary to replace the Hookean springs of Rouse theory, with finitely extensible springs, to capture certain observed features, such as the shear thinning exhibited by the shear viscosity, and the boundedness of the elongational viscosity,[6] that are a consequence of the finite contour length of the polymer molecule. Several theoretical papers,[7−9] published after the experiments of Smith and Chu, have used some or all of these phenomena in their models and have shown that obtaining quantitative comparison with the DNA stretch measurements requires the inclusion of all these three phenomena.

The incorporation of each of these phenomena leads to the introduction of at least one new parameter into the theory. For instance, the pairwise strength of excluded-volume interactions between any two beads in the bead−spring chain is typically represented by the nondimensional parameter z^*, which is proportional to $(1 - T_\theta/T)$, where T is the solution temperature and T_θ is the θ-temperature of the polymer−solvent system. The strength of hydrodynamic interactions, on the other hand, which arise due to the hydrodynamic drag experienced by the beads, is usually measured in terms of the magnitude of the parameter h^*, the nondimensional bead radius. Finally, the inclusion of finitely extensible springs introduces the parameter b, which is a nondimensional measure of the fully stretched length of a spring. Not surprisingly, for any particular choice of the number of beads N, a proper choice of the values of these parameters turns out to have a crucial bearing on the accuracy of the predictions of the various theories. All the previously mentioned papers[7−9] determine the correct values of the parameters to use in their simulations, by essentially finding a best fit to experimental data, in some limiting regime of behavior. For instance, Jendrejack et al. simultaneously obtain all three pa-

* Author to whom correspondence should be adressed. E-mail: Ravi.Jagadeeshan@eng.monash.edu.au.

10.1021/ma0359411 CCC: $30.25
Published on Web 12/15/2004

rameters, z^*, h^*, and b, by fitting model predictions to experimentally reported observations of equilibrium λ-phage DNA stretch, relaxation time, and diffusivity.[8] Larson and co-workers, on the other hand, exploit the expectation that a polymer coil will unravel into a fully stretched state at high enough strains and consequently behave like a long slender cylindrical rod to estimate h^*. They neglect the presence of excluded-volume interactions (which corresponds to setting $z^* = 0$) and obtain the parameter b from reported estimates of the number of Kuhn steps, N_k, for λ-phage DNA. Though the procedure of Jendrejack et al. is a reasonable scheme for parameter estimation, it is not clear that the chosen set of values is unique and that an alternative set of parameter values will not yield equally accurate predictions of either equilibrium properties or the extent of stretch in extensional flow. Furthermore, a simultaneous fit of all the parameters to experimental results does not recognize the fact that a few of the parameters have no influence on some of the experimental variables. For instance, the parameter h^* has no influence on the equilibrium stretch of λ-phage DNA. The parameter estimation procedure of Larson and co-workers leads to accurate predictions of the stretch at moderate to high values of the Hencky strain. However, it leads to a poor prediction of the stretch at low strains.

The aim of the present work, as in the case of the earlier theoretical efforts cited above, is to examine the relative importance of various nonlinear effects in determining the evolution of DNA stretch in extensional flow. The problem of parameter estimation is approached here, however, within the broader context of the universal behavior exhibited by dilute polymer solutions, both at and close to equilibrium. In particular, an attempt is made to bring the significant insight that has been gained in recent years into the proper treatment of hydrodynamic and excluded-volume interaction effects in dilute polymer solutions to bear on the problem of DNA conformational evolution prediction.

To elucidate the current understanding of the role of solvent mediated interactions (HI and EV) in determining the dynamics of polymer solutions, it is necessary to distinguish between the behavior of θ-solvents and good solvents and further between experimental observations and theoretical results.

For any observed dynamic property $\phi^{\theta}_{\mathrm{exp}}$ in a θ-solution, one can construct a nondimensional ratio

$$U^{\theta}_{\phi,\mathrm{exp}} = \frac{\phi^{\theta}_{\mathrm{exp}}}{g(R^{\theta}_{\mathrm{g,exp}})} \tag{1}$$

where $R^{\theta}_{\mathrm{g,exp}}$ is the experimentally measured radius of gyration in a θ-solvent and g is a function of $R^{\theta}_{\mathrm{g,exp}}$, such that it has the same dimensions and scaling with molecular weight, M, as $\phi^{\theta}_{\mathrm{exp}}$. Experimental observations indicate that for a very large number of polymer−solvent systems the ratio $U^{\theta}_{\phi,\mathrm{exp}}$ attains a universal value, independent of molecular weight and chemistry, by relatively small values of M (of order 10 000). An example of such a universal ratio is the well-known Flory constant, which is a nondimensional function of the intrinsic viscosity and the radius of gyration. Thus, the magnitude of any dynamic property $\phi^{\theta}_{\mathrm{exp}}$, for a linear flexible polymer molecule with radius of gyration $R^{\theta}_{\mathrm{g,exp}}$, can be simply obtained from eq 1, provided one knows the universal value $U^{\theta}_{\phi,\mathrm{exp}}$.

The important role played by hydrodynamic interactions in θ-solutions is made evident by the fact that universal ratios involving dynamic properties, as discussed above, can be shown to exist theoretically only when HI effects are incorporated. Both approximate analytical theories, and more recent exact Brownian dynamics simulations, have shown that the strength of HI for a polymer−solvent system at equilibrium, or close to equilibrium, is measured by the magnitude of the draining parameter, $h \equiv h^*\sqrt{N}$, and various nondimensional ratios of equilibrium and linear viscoelastic properties attain constant universal values in the nondraining limit $h \rightarrow \infty$.[10] The experimental observation that universal values are obtained by relatively small values of M indicates that most systems reach the nondraining limit for relatively small values of h (since h is proportional to the square root of molecular weight). Recently, Kröger et al.[11] have established the methodology for obtaining exact predictions of universal ratios in the nondraining limit (within simulation error bounds) from Brownian dynamics simulations. By accumulating data for finite values of N, at various constant values of h^*, they show that the values of a host of universal ratios, obtained by extrapolating finite chain data to the limit $N \rightarrow \infty$, are unique, independent of the particular choice of h^* and reasonably close to experimentally measured values. Thus, provided one is in the nondraining limit, the precise value of h^* used to get there is immaterial.

Experimental observations of the static behavior of polymer solutions under good solvent conditions have shown that while both the deviation of the solution temperature T, from the θ-temperature T_θ, and the molecular weight M determine the "goodness" of the solvent, they can be combined into an unique quantity called the solvent quality, $z = v_0(1 - T/T_\theta)\sqrt{M}$, where v_0 is a constant, such that master plots of the dependence of material properties on solvent quality, for a variety of polymer−solvent systems, can be constructed when plotted in terms of z. Thus, for any observed property ϕ_{exp}, the ratio $\alpha_\phi = \phi_{\mathrm{exp}}/\phi^{\theta}_{\mathrm{exp}}$ has been shown to be a universal function of z, $\alpha_\phi = \alpha_\phi(z)$. A well-known example of such a function is the swelling of the polymer chain α_g, defined as the ratio of the radius of gyration R_g in a good solvent to the radius of gyration in a θ-solvent, which can be shown to be a universal function of z.[12] Thus, provided the universal properties $U^{\theta}_{\phi,\mathrm{exp}}$ and $\alpha_\phi(z)$ are known, the magnitude of any material property ϕ_{exp}, for a polymer−solvent system under good solvent conditions, can be determined, given $R^{\theta}_{\mathrm{g,exp}}$ and z.

Approximate analytical theories for excluded-volume effects in dilute polymer solutions[10,13] have shown that the correct theoretical estimate of solvent quality is given by the expression $z = z^*\sqrt{N}$. Furthermore, theoretical predictions can be mapped onto the experimentally observed universal dependence of material properties on z by making a suitable choice of the constant v_0. Recently, Kumar and Prakash[14] have shown that by using a narrow-Gaussian potential, and adopting a finite chain data extrapolation procedure similar to that of Kröger et al., accurate predictions of universal crossover scaling functions, free of any approximations, can be obtained by carrying out Brownian dynamics simulations.

Since Kumar and Prakash neglect hydrodynamic interactions, they obtain predictions of only static properties. However, by combining the approach of Kröger et al. and Kumar and Prakash, the coupled influence of HI and EV effects on universal properties can now be explored. It is worthwhile to note that both the procedures of Kröger et al. and Kumar and Prakash require the extrapolation of finite chain data to the long chain limit, $N \rightarrow \infty$. The limiting process is, however, carried out by simultaneously letting both the length of a single spring and z^* tend to zero such that R_g^θ and z remain constant. Interestingly, while results obtained in the limit $N \rightarrow \infty$ imply that the contour length of the polymer chain is infinite, they can still be used to describe polymer−solvent systems with a finite molecular weight since both the radius of gyration R_g^θ and the solvent quality z are kept finite. In brief, the central conclusion of the discussion of HI and EV above is that (i) most polymer−solvent systems at equilibrium, or close to equilibrium, approach the nondraining limit for relatively small values of h and (ii) the quality of the solvent can be characterized by a single variable z. Furthermore, accurate predictions in the universal regime, of all static and dynamic properties of a dilute polymer solution, characterized by specific values of R_g^θ and z, can be obtained, independent of model parameters, by extrapolating appropriate results of bead−spring chain models to the limit $N \rightarrow \infty$.

Recent investigations have shown that the general methodology of extrapolating finite bead−spring chain data to the long chain limit, to obtain predictions of the universal behavior of dilute polymer solutions, can also be extended to shear flows far from equilibrium.[15−17] It has been found that in this case master plots are obtained when the dependence on the shear rate $\dot{\gamma}$ is interpreted in terms of the characteristic shear rate, $\beta = [\eta]_0 M \eta_s \dot{\gamma}/RT$, where η_s is the solvent viscosity, $[\eta]_0$ is the zero shear rate intrinsic viscosity, and R is the gas constant. As in the equilibrium and linear viscoelastic regimes, predictions in the asymptotic limit are obtained while keeping z, R_g^θ, and β constant.

The universal behavior that is predicted in each of these situations is now well understood to have its origins in the self-similar nature of long chain flexible macromolecules in the coiled state. As more and more springs are included in the bead−spring chain, local details of the chain are masked from the flow, leading to parameter-free predictions. The use of infinitely extensible Hookean springs in the model does not impose any constraint on the contour length of the chain, which, as mentioned earlier, tends to infinity.

It is natural to attempt to extend these ideas to the case of extensional flows. However, polymer molecules do not always remain coiled in an extensional flow. As is well-known, in terms of the nondimensional Weissenberg number Wi (defined by $Wi = \lambda\dot{\epsilon}$, where λ is a time constant characteristic of the large scale relaxation of the polymer and $\dot{\epsilon}$ is the extensional rate), for values of $Wi \gtrsim Wi_c$, where Wi_c is a critical Weissenberg number (whose numerical value depends on the choice of λ), the polymer molecule is unravelled from a coillike state to a fully stretched rodlike state, as the Hencky strain, $\epsilon = \dot{\epsilon}t$, increases. The coil−stretch transition occurs because of the finite length of the molecule. In the stretched state, it is clear that universal behavior will not be observed since the local details of the polymer are completely exposed to the flow. On the other hand, for $Wi < Wi_c$ and even in the case where $Wi \gtrsim Wi_c$, for some range of strain values, universal behavior may be expected for sufficiently long polymer chains. The aim of this work is to carefully examine this question, in the context of the conformational evolution of λ-phage DNA, and determine the regime of behavior where the ideas of universality may be applied to extensional flows.

This task immediately raises a fundamental issue. It is well-known that Hookean springs cannot be used to describe extensional flows because they lead to unbounded steady-state predictions for $Wi \gtrsim Wi_c$. As mentioned earlier, previous theoretical attempts have shown that finitely extensible springs, with the appropriate force law, can be used successfully to describe the entire range of behavior. The question that naturally arises in this context is, how should the procedure for obtaining predictions in the presence of HI and EV, discussed above for models with Hookean springs, be revised for a model with finitely extensible springs? In other words, (i) what measure of HI should be held constant as N is increased so as to approach the nondraining limit, and (ii) how can a constant solvent quality be maintained in the course of this procedure? The resolution of these issues forms the foundation for the present work. We show that, even in the presence of finitely extensible springs, it is possible to make use of the insight gained earlier with Hookean springs. Once the revised procedure is established, we show that the regime of applicability of the concepts of universality can be examined unambiguously.

After reviewing the necessary formalism for the model and its parameters in section 2, we present a fairly detailed discussion of the existing approaches to parameter estimation and show how it is possible to exploit the existence of universal behavior to address the problem of parameter estimation in section 3. The systematic procedure that is developed as a consequence, for the treatment of finite chains, which is termed here as successive fine graining (SFG), is discussed in section 4. The universal stretch experienced by a polymer chain in uniaxial extensional flow and the departure from universal behavior by finite chains are discussed in section 5. The estimation of parameters within this framework, for λ-phage DNA, using available experimental measurements, is given in section 6.1. Finally, the theoretical prediction of the conformations of DNA molecules in elongational flow and a comparison of predictions with experiments are given in section 6.2.

2. Bead−Spring Chain Model

In this work, as mentioned earlier, a dilute solution of DNA molecules is modeled as an ensemble of noninteracting bead−spring chains, each of which has N beads (which act as centers of hydrodynamic resistance) connected by massless springs representing an entropic force between two points on the polymer chain. If $\psi(\mathbf{r}_1,...,\mathbf{r}_N)$, is the configurational distribution function of the bead positions $\mathbf{r}_\mu$, then the starting point in any statistical theory of bead−spring chains is the "diffusion" equation or Fokker−Planck equation for the evolution of ψ:[5,6,18]

$$\frac{\partial \psi}{\partial t} = -\sum_{\mu=1}^{N} \frac{\partial}{\partial \mathbf{r}_\mu} \cdot \left[\kappa \cdot \mathbf{r}_\mu + \frac{1}{\zeta} \sum_{\nu=1}^{N} \mathbf{\Gamma}_{\mu\nu} \cdot (\mathbf{F}_\nu^s + \mathbf{F}_\nu^{int}) \right] \psi + \frac{kT}{\zeta} \sum_{\mu,\nu=1}^{N} \frac{\partial}{\partial \mathbf{r}_\mu} \cdot \mathbf{\Gamma}_{\mu\nu} \cdot \frac{\partial \psi}{\partial \mathbf{r}_\nu} \quad (2)$$

Here, κ is a time-dependent, homogeneous, velocity gradient tensor of the surrounding fluid motion, ζ is the hydrodynamic friction (drag) coefficient associated with the bead, k is Boltzmann's constant, and $\mathbf{\Gamma}_{\mu\nu}$ is the hydrodynamic interaction tensor, representing the effect of the motion of a bead μ on another bead ν through the disturbances carried by the surrounding fluid. $\mathbf{F}^{\mathrm{s}}_{\nu}$ is the entropic spring force on bead ν due to adjacent beads, $\mathbf{F}^{\mathrm{s}}_{\nu} = \mathbf{F}^{\mathrm{c}}(\mathbf{Q}_{\nu}) - \mathbf{F}^{\mathrm{c}}(\mathbf{Q}_{\nu-1})$, where $\mathbf{F}^{\mathrm{c}}(\mathbf{Q}_{\nu-1})$ is the force between the beads $\nu - 1$ and ν, acting in the direction of the connector vector between the two beads $\mathbf{Q}_{\nu} = \mathbf{r}_{\nu} - \mathbf{r}_{\nu-1}$. The quantity $\mathbf{F}^{\mathrm{int}}_{\mu}$ is the sum total of the remaining interaction forces on bead μ due to all other beads, $\mathbf{F}^{\mathrm{int}}_{\mu} = \sum_{\nu=1}^{N}\mathbf{F}^{\mathrm{e}}(\mathbf{r}_{\mu\nu})$, where $\mathbf{F}^{\mathrm{e}}$ is the binary force acting along the vector $\mathbf{r}_{\mu\nu} = \mathbf{r}_{\nu} - \mathbf{r}_{\mu}$ connecting beads μ and ν. In the case of DNA we assume that this force is derived from a purely repulsive potential representing excluded-volume effects.

Specifying the exact nature of the forces and the hydrodynamic interaction tensor completes the model. The simplest realization of this model is the Rouse chain with a Hookean (linear) spring force and no other forces arising due to excluded-volume or hydrodynamic interactions. However, as discussed earlier, it is essential to include a nonlinear spring force, hydrodynamic interactions, and excluded-volume effects in order to capture many of the features of dilute solution behavior. For DNA a commonly employed spring model is a wormlike chain (WLC) force "law" which is an interpolatory formula between the limits of the Hookean (linear) regime and the fully stretched singular regime[19]

$$\mathbf{F}^{\mathrm{c}}_{\mathrm{WLC}}(\mathbf{Q}) = H\mathbf{Q}\,\frac{1}{6q}\left(4q + \frac{1}{(1-q)^2} - 1\right) \tag{3}$$

where H is the linear spring constant and $q = Q/Q_0$ is the ratio of the magnitude of the connector vector Q and the fully stretched length Q_0. With regard to the EV effects, recent simulations[14] with Hookean springs have shown that with the help of a narrow-Gaussian excluded-volume potential the universal equilibrium crossover behavior of dilute polymer systems can be accurately predicted. The advantages of using this potential are (a) it reduces to the δ-function potential in an appropriate limit, (b) it permits a simple calculation of terms in a perturbation expansion, and (c) it is also computationally easy to handle. It is written as a regularization of a the δ-function potential:[20,21]

$$\phi^{\mathrm{e}}(r) = \frac{kTv}{(2\pi d^2)^{3/2}}\,\mathrm{e}^{-r^2/2d^2} \tag{4}$$

where v is the excluded-volume parameter and d is a parameter that specifies the range of interaction. The excluded-volume force between beads separated by a distance $\mathbf{r}$ is hence given by

$$\mathbf{F}^{\mathrm{e}}(\mathbf{r}) = -\frac{\partial\phi^{\mathrm{e}}}{\partial\mathbf{r}} = kT\,\frac{v}{(2\pi)^{3/2}d^5}\,\mathrm{e}^{-r^2/2d^2}\,\mathbf{r} \tag{5}$$

In eq 2, the hydrodynamic interaction tensor $\mathbf{\Gamma}_{\mu\nu}$ is written in general as

$$\mathbf{\Gamma}_{\mu\nu} = \delta_{\mu\nu}\boldsymbol{\delta} + \zeta\mathbf{\Omega}_{\mu\nu} \tag{6}$$

where $\mathbf{\Omega}_{\mu\nu}$, for $\mu \neq \nu$, represents the actual interaction matrix, and $\boldsymbol{\delta}$ and $\delta_{\mu\nu}$ represent a unit tensor and a Kronecker delta, respectively. For theoretical analyses, it is usually convenient to use the Oseen–Burgers function for the tensor $\mathbf{\Omega}_{\mu\nu} = \mathbf{\Omega}(\mathbf{r}_{\mu\nu})$, where the functional form, $\mathbf{\Omega}(\mathbf{r})$, is given by[18]

$$\mathbf{\Omega}(\mathbf{r}) = \frac{1}{8\pi\eta_{\mathrm{s}}r}\left(\boldsymbol{\delta} + \frac{\mathbf{rr}}{r^2}\right) \tag{7}$$

In the simulations employed later in this paper, however, we have used the regularized form given by the Rotne–Prager–Yamakawa (RPY) interaction tensor.[22,23] The expression for the RPY tensor is given in a nondimensional form shortly below.

It is convenient to render the equations dimensionless. For a Hookean spring $\sqrt{kT/H}$ is its characteristic length at equilibrium, and $(\zeta/4H)$ is the characteristic relaxation time of a single spring (in other words the relaxation time for a dumbbell), in the absence of hydrodynamic interactions. Choosing these to be the reference length scale $l_{\mathrm{H}} \equiv \sqrt{kT/H}$ and time scale $\lambda_{\mathrm{H}} \equiv \zeta/4H$, the dimensionless form of the various governing equations are given below.

The nondimensional spring force is given by

$$\mathbf{F}^{\mathrm{c}}_{\mathrm{WLC}}(\mathbf{Q}^*) = \mathbf{Q}^*\,\frac{1}{6q^*}\left(4q^* + \frac{1}{(1-q^*)^2} - 1\right) \tag{8}$$

where $q^* = Q^*/\sqrt{b}$ and $b = Q_0{}^2/l_{\mathrm{H}}{}^2$. The excluded-volume force becomes

$$\mathbf{F}^{\mathrm{e}}(\mathbf{r}^*) = \frac{z^*}{d^{*5}}\,\mathrm{e}^{-r^{*2}/2d^{*2}}\,\mathbf{r}^* \tag{9}$$

where the nondimensional parameters are $z^* = v/(2\pi l_{\mathrm{H}}{}^2)^{3/2}$ and $d^* = d/l_{\mathrm{H}}$. The hydrodynamic interaction function given by the Rotne–Prager–Yamakawa regularization of the Oseen function in terms of nondimensional variables is

$$\mathbf{\Omega}(\mathbf{r}^*) = \left[\Omega_1\boldsymbol{\delta} + \Omega_2\frac{\mathbf{r}^*\mathbf{r}^*}{r^{*2}}\right] \tag{10}$$

where for $r^* \geq 2\sqrt{\pi}h^*$

$$\Omega_1 = \frac{3\sqrt{\pi}}{4}\frac{h^*}{r^*}\left(1 + \frac{2\pi}{3}\frac{h^{*2}}{r^{*2}}\right),$$
$$\Omega_2 = \frac{3\sqrt{\pi}}{4}\frac{h^*}{r^*}\left(1 - 2\pi\frac{h^{*2}}{r^{*2}}\right) \tag{11}$$

and for $0 < r^* \leq 2\sqrt{\pi}h^*$

$$\Omega_1 = 1 - \frac{9}{32}\frac{r^*}{h^*\sqrt{\pi}}, \quad \Omega_2 = \frac{3}{32}\frac{r^*}{h^*\sqrt{\pi}} \tag{12}$$

The quantity h^* has been introduced previously as the nondimensional radius of the bead. It is also known as the hydrodynamic interaction parameter and is defined by

$$h^* \equiv \frac{a}{\sqrt{\pi}l_{\mathrm{H}}} \tag{13}$$

The above expressions reduce to the corresponding expressions for the Oseen tensor in the limit of $r^* \gg$

h^*. In deriving the above expressions, the Stokes drag formula $\zeta = 6\pi\eta_s a$ for a spherical bead of radius a has been used. With these redefined expressions, the nondimensional diffusion equation can be written as

$$\frac{\partial\psi}{\partial t^*} = \sum_{\mu,\nu=1}^{N} \frac{\partial\psi}{\partial \mathbf{r}^*_\mu} \cdot \mathbf{\Gamma}_{\mu\nu}(h^*) \cdot \frac{\partial\psi}{\partial \mathbf{r}^*_\nu} - \sum_{\mu=1}^{N} \frac{\partial\psi}{\partial \mathbf{r}^*_\mu} \cdot \left[\kappa^* \cdot \mathbf{r}^*_\mu + \sum_{\nu=1}^{N} \mathbf{\Gamma}_{\mu\nu}(h^*) \cdot \left(\mathbf{F}^s_\nu(b) + \mathbf{F}^{int}_\nu(z^*, d^*)\right)\right]\psi \quad (14)$$

where the parameter dependence for the functions has been retained to show their explicit occurrence, and the forces are to be understood as having been nondimensionalized by $\sqrt{HkT}$.

The exact solution of the time evolution of various averages carried out with the distribution function ψ, without any further approximations, can be obtained by writing a stochastic differential equation (SDE) equivalent to eq 14 and solving it with the help of a Brownian dynamics algorithm.[18] In the presence of fluctuating HI, the problem of the computational intensity of calculating the Brownian term has been attenuated significantly recently[23] by the use of a Chebyshev polynomial representation[24] for the Brownian term. We have adopted this strategy, and the details of the exact algorithm followed here are given in ref 25.

3. Model Parameters

One of the main aims of this paper is to examine the region in Weissenberg number and Hencky strain space, in which a parameter-free prediction of the conformational evolution of λ-DNA can be made. The general procedure is to determine the model parameters such that the model correctly reproduces known equilibrium properties of the chain. Once this is done, predictions in elongational flow at any deformation rate are then obtained. The procedure followed in ref 8 is similar in spirit to this approach. However, as mentioned earlier, the procedure given in ref 9, though novel, adopts a different strategy which does not require conformation to equilibrium properties. The emphasis in the present work is to determine the parameters that yield the correct equilibrium properties, while at the same time being consistent with our current understanding of the role of HI and EV effects. In this spirit, a detailed discussion of the model parameters and their influence on equilibrium properties is taken up below. It is worthwhile to note that the arguments are not specific to DNA alone and might be applied to any long-chain flexible macromolecule.

The theoretical prediction of any dimensional physical property ϕ of the polymer solution is obtained by carrying out a suitable configurational average with the distribution function ψ, which satisfies the diffusion equation, eq 14. The property can then be represented as a function of nondimensional model parameters, in the general form

$$\phi = \phi^*(N, h^*, b, z^*, d^*)\, S(l_H, \lambda_H) \quad (15)$$

where S is the corresponding function that provides the dimensions. Since l_H and λ_H are the reference length and time scales for the nondimensional model, they do not alter the model variable ϕ^*. However, unlike many problems in physics where a measurable quantity is used for the purposes of nondimensionalization, l_H and λ_H are quantities that are completely intrinsic to the bead−spring model and are not experimentally observable. Therefore, to make a dimensional comparison of the model predictions with experimental measurements, it is essential to fix l_H and λ_H by matching dimensional model variables with some suitable choice of experimental quantities, as discussed in greater detail below.

3.1. Parameter Determination at Equilibrium. In this section we discuss some possible procedures, along the lines previously suggested by Öttinger,[26] that might be adopted for a systematic determination of the parameters for any polymer−solvent system, including that of λ-phage DNA. As will be seen shortly, this will turn out to be quite a difficult task and will serve as a motivation both for the procedures that are currently adopted and for the procedure suggested in our work.

3.1.1. Free Draining Hookean Springs at θ-Conditions To illustrate a simple case of parameter determination, we consider the Rouse model, which has Hookean springs ($b \to \infty$), is free-draining ($h^* = 0$), and is under θ-conditions ($z^* = 0$, $d^* = 0$). Therefore, the only parameters are $\{l_H, \lambda_H, N\}$, in which N is arbitrary, while the remaining two can be determined given two experimental measurements. The general procedure is to match some characteristic experimental size and time constant to the corresponding values obtained from the model. If the experimentally observed radius of gyration $R^\theta_{g,exp}$ is known, then for any given N the dimensional radius of gyration of the model is $R^\theta_{g,mod} = R^*_g(N) l_H$, where $R^*_g(N)$ is the nondimensional model value for the given value of N. For Hookean bead−spring chains of a given N, $R^{*2}_g = (N^2 - 1)/(2N)$; thus, l_H is determined by matching $R^\theta_{g,mod}$ with $R^\theta_{g,exp}$

$$l_H = \frac{R^\theta_{g,exp}}{R^*_g} \quad (16)$$

Similarly, let λ_{exp} be some characteristic macroscopic time constant measured experimentally (such as the longest relaxation time or a time derived from the intrinsic viscosity or the diffusivity). For example, in the case of the relaxation time constructed from the intrinsic viscosity $[\eta]_0$, we have[5]

$$\lambda_{exp} = \lambda_\eta \equiv \frac{[\eta]_0 M}{N_A} \frac{\eta_s}{kT} \quad (17)$$

where N_A is the Avogadro number. Equating the relaxation time from the model $\lambda_{mod} = \lambda^*(N)\, \lambda_H$ to the experimental relaxation time λ_{exp}, the reference time λ_H can be fixed. In the case of a Rouse model, $\lambda^*(N)$ is straightforward to calculate.

3.1.2. Hookean Springs with HI at θ-Conditions. In the case of a model with HI, the scheme for the determination of the length scale remains the same, since inclusion of hydrodynamic interaction does not alter static properties. However, the characteristic time from the model now has an additional dependence on the parameter h^* expressed as $\lambda^*(N,h^*)$, and the determination of h^* and λ_H is coupled due to the relationship

$$\lambda_H = \frac{6\pi\eta_s a}{4H} = \frac{\eta_s}{kT} \frac{3}{2} \pi^{3/2} {l_H}^3 h^* \quad (18)$$

It is to be noted that it is not required to actually measure λ_{exp}, since it is known that for a polymer with

a sufficiently large molecular weight the time constant is related to the macroscopic size by an universal constant. For example, a relaxation time can be related to the radius of gyration by

$$\lambda_{\mathrm{exp}} = \frac{\eta_{\mathrm{s}}}{kT}\frac{4\pi}{3}(R^{\theta}_{\mathrm{g,exp}})^3 U^{\mathrm{exp}}_{\lambda\mathrm{R}} \tag{19}$$

where $U^{\mathrm{exp}}_{\lambda\mathrm{R}}$ is a known universal constant. For instance, the universal number corresponding to λ_{η}, denoted here by $U_{\eta\mathrm{R}}$ (which is equivalent to the Flory–Fox parameter Φ), is given by

$$U_{\eta\mathrm{R}} = \frac{9\sqrt{6}}{2\pi}\frac{\Phi}{N_{\mathrm{A}}} = 1.45 \tag{20}$$

based on the reported[27] value of $\Phi = 2.5 \times 10^{23}$. Consequently, all quantities on the rhs of eq 19 are experimentally measurable, and the universal number is also known for a given choice of λ.

Using eqs 18 and 19 and the fact that l_{H} has already been determined by matching with $R^{\theta}_{\mathrm{g,exp}}$, we obtain

$$\frac{9\sqrt{\pi}}{8}h^*\frac{\lambda^*(N,h^*)}{R^{*3}_{\mathrm{g}}(N)} = U^{\mathrm{exp}}_{\lambda\mathrm{R}} \tag{21}$$

which is a nonlinear algebraic equation in the unknowns N and h^*. For a given choice of N, eq 21 needs to be solved for the value of h^*, and subsequently eq 18 can be used to determine λ_{H}. There is no closed form solution to this equation for a model which includes fluctuating HI. However, it is well-known that with the preaveraging approximation for HI it is possible to analytically obtain the solution to $\lambda^*(N,h^*)$ by solving an eigenvalue problem.[28] It is also known that a value of $h^* \approx 0.24$ provides a uniformly good approximation to the solution of eq 21 for $N \gg 1$.[29] It will be shown later that this approximation is not always true when finitely extensible springs are used instead of Hookean springs.

3.1.3. Combined Effects Including Finite Extensibility The results obtained so far are valid only for a chain of Hookean springs. As mentioned earlier, such a chain will not be a useful approximation in most strong flow situations, and the finite length of the polymer has to be incorporated (i.e., the parameter b, defined below eq 8, will have a finite value). In this case the determination of the length scale l_{H} and the parameter b are coupled and require an additional experimental measurement, namely, the fully stretched length of the polymer denoted by $L_{0,\mathrm{exp}}$. The fully stretched length of the bead spring chain is given by

$$L_{0,\mathrm{mod}} = (N-1)\sqrt{b}\,l_{\mathrm{H}} \tag{22}$$

Note that the static properties at equilibrium are also functions of b. For instance, the radius of gyration is given by

$$(R^{\theta}_{\mathrm{g,mod}})^2 = \chi^2(b)\frac{N^2-1}{2N}{l_{\mathrm{H}}}^2 \tag{23}$$

where $\chi(b)$ is a known function of b for a given spring force model (see Appendix A for further details). This leads to two simultaneous equations in the unknowns l_{H} and b, from which the solution for b can be formally written as

$$\frac{b}{\chi^2(b)} = \frac{{L_{0,\mathrm{exp}}}^2}{(R^{\theta}_{\mathrm{g,exp}})^2}\frac{N+1}{2N(N-1)} \equiv N_{\mathrm{k}}\frac{3(N+1)}{N(N-1)} \tag{24}$$

where it is to be understood that the corresponding experimental ratio has been used in place of the model ratio. In eq 24, we have also used the definition

$$N_{\mathrm{k}} \equiv \frac{{L_{0,\mathrm{exp}}}^2}{6(R^{\theta}_{\mathrm{g,exp}})^2} \tag{25}$$

where N_{k} is the number of Kuhn statistical segments (or Kuhn steps) in an equivalent bead–rod model.[6] Once b is determined, and therefore the value of χ, l_{H} can be determined as before, but in this case by using eq 23 for the radius of gyration obtained with finitely extensible springs.

The problem of fixing λ_{H} and h^*, however, becomes considerably more difficult, since for finite N even the preaveraging approximation is difficult to solve; i.e., an equation similar to eq 21 must be solved with a function $\lambda^*(N,h^*,b)$. Hsieh et al.[9] have suggested a novel procedure to estimate the value of h^*, namely, by matching the drag from a fully extended spring to that of a slender rod. However, this does not ensure that the relaxation time of the model matches the experimental value. In Appendix A we show that by using a preaveraging approximation it is possible to obtain an approximate solution of this equation, similar to that obtained in ref 29 for Hookean springs.

With the need to incorporate good solvent effects through the excluded-volume potential, two more parameters, z^* and d^*, enter both the size R^*_{g} and the time constant $\lambda^*(N,h^*,b,z^*,d^*)$. This problem is difficult even when considering Hookean springs. There is no systematic procedure to obtain these parameters, and because of this difficulty, it is not clear how many more experimental measurements are required to determine the parameters. It is not surprising, therefore, that within this framework of parameter estimation the best option might be to simply adopt a parameter fitting procedure to all the available experimental data for DNA, as has been pursued in ref 8.

The difficulties associated with the approach suggested above for parameter estimation can be summarized as (a) the arbitrariness in the choice of number of beads N, (b) the failure to isolate the effects of HI and EV, and (c) the failure to incorporate the existence of a unique relationship between the size (static) and time (dynamic) constants of long-chain polymers, thereby requiring several additional experimental measurements to determine the model length scales, time scales, and parameters. In the following, we show how these drawbacks can be overcome by exploiting the universal behavior of bead–spring chain models to obtain the model parameters with minimal experimental measurements.

3.2. Parameter-Free Predictions for a Chain of Hookean Springs at Equilibrium. Insofar as purely equilibrium properties are concerned, where the finite length of the molecule is not a concern, we can use a chain of Hookean springs to represent the long chain polymer molecule, as is commonly done in most theoretical treatments.[5] This will provide a good illustration of the method to obtain parameter-free predictions, which can then be carried over to a chain with finitely extensible springs. The general principle behind the

following analysis is to exploit the universal behavior of long chain polymers, which will remove the arbitrariness in the choice of N. We first reconsider the case of a solution under θ-conditions, with the idea being to isolate the parameter estimation procedure for HI and EV effects.

3.2.1. Polymer Solution under θ-Conditions. Since Hookean springs are used, the procedure for determining l_H is still the same as discussed in section 3.1.1, i.e., by matching $R^\theta_{g,mod}$ to $R^\theta_{g,exp}$. However, the matching of time constants is done by a different procedure. As mentioned earlier, the unique behavior exhibited by solutions of long chain polymers is the universality observed in experiments, which relates static properties to dynamic ones through a universal ratio.[30] This is represented in general by eq 1 and illustrated in a particular case by eq 19. For a chain of Hookean springs, we can define a similar ratio with model variables

$$U^\theta_{\phi,mod} \equiv \frac{\phi^\theta_{mod}}{g(R^\theta_{g,mod})} \tag{26}$$

Since $U^\theta_{\phi,mod}$ is nondimensional, we can write it in terms of the model parameters as $U^\theta_{\phi,mod} = U^\theta_{\phi,mod}(N,h^*)$. As discussed previously, the value of this ratio in the nondraining limit approaches a constant value, independent of h^*. This has recently been demonstrated for several ratios using simulations with fluctuating HI,[11] where independence from the value chosen for h^* was observed as $N \to \infty$. Both approximate analytical theories and simulations results have shown that the asymptotic behavior of this ratio can be expressed in a general form as

$$U^\theta_{\phi,mod}(N,h^*) = U^\infty_\phi + c_\phi\left(\frac{1}{h^*} - \frac{1}{h^*_f}\right)\frac{1}{\sqrt{N}} + \mathcal{O}\left(\frac{1}{N}\right) \tag{27}$$

where U^∞_ϕ is the asymptotic value and c_ϕ is a constant. The leading order correction to the limiting value was shown to be $\mathcal{O}(1/\sqrt{N})$ in the Zimm theory[29] as well as in simulations.[11] The quantity h^*_f is also a constant, which is typically called the fixed point. It has a special significance, as is evident from eq 27: For the choice $h^* = h^*_f$, the leading order correction to the limiting value changes from being of $\mathcal{O}(1/\sqrt{N})$ to $\mathcal{O}(1/N)$. Thus, the asymptotic value U^∞_ϕ, which is attained in the nondraining limit $h \to \infty$, is reached for smaller values of N.

Combining eqs 1 and 27, we have for any dynamic property obtained from the model, in the limit of $N \to \infty$

$$\phi^\theta_\infty \equiv \lim_{N\to\infty} \phi^\theta_{mod}(N, h^*, l_H, \lambda_H) = \phi^\theta_{exp}\frac{U^\infty_\phi}{U^\theta_{\phi,exp}}\frac{g(R^\theta_{g,mod})}{g(R^\theta_{g,exp})} \tag{28}$$

Since for a given value of N, $R^\theta_{g,mod}$ is matched to the experimental value $R^\theta_{g,exp}$, this equation implies that the model prediction for any dynamic property reaches an asymptotic value ϕ^θ_∞, irrespective of h^*. Moreover, it has been shown[11] that the simulation values for the universal constants (U^∞_ϕ) agree very closely with the experimental value ($U^\theta_{\phi,exp}$) for several dynamic properties. Therefore, in the limit of $N \to \infty$ the value ϕ^θ_∞ automatically agrees with the experiment value ϕ^θ_{exp}, for any value of the parameter h^*. The important difference between this approach and the finite N method discussed earlier is that it is no longer necessary to solve an equation like eq 21 to obtain h^*; any reasonable value will suffice. For this choice of h^*, the time scale λ_H is determined from eq 18.

In practice, the asymptotic value ϕ^θ_∞, for models with fluctuating HI, is typically obtained using the following procedure. The ratio $U^\theta_{\phi,mod}(N,h^*)$ is calculated by carrying out simulations, with h^* kept constant, for increasing values of N. The limiting value U^∞_ϕ is then obtained by plotting the finite chain simulation values vs $1/\sqrt{N}$ and extrapolating to the limit $N \to \infty$. Finally, ϕ^θ_∞ is obtained by using the expression $\phi^\theta_\infty = U^\infty_\phi g(R^\theta_{g,mod})$. While physically meaningful values of h^* lie in the range $0 < h^* < 0.5$,[26] it has been shown that a value in the range $0.20 < h^* < 0.25$ provides better convergence even at small values of N, since $h^*_f \approx 0.24$.[11]

3.2.2. Polymer under Good-Solvent Conditions Now we consider a chain which includes excluded-volume effects to model a polymer dissolved in a good solvent at equilibrium. As mentioned earlier, it has been experimentally observed that the temperature and molecular weight dependence of any macroscopic property ϕ under good solvent conditions (for various polymer−solvent systems, molecular weights, and temperatures) can be collapsed on to a master curve,[12] which can be expressed as

$$\phi = \phi^\theta_{exp}\alpha_\phi(z) \tag{29}$$

where ϕ^θ_{exp} is the value of the same property under θ-conditions and z is the solvent quality defined by $z = v_0\,(1 - T/T_\theta)\sqrt{M}$, where v_0 is a chemistry-dependent constant used to shift the curves on to the master curve, $\alpha_\phi(z)$. Since it has also been observed that all macroscopic properties under θ-conditions can be related to the $R^\theta_{g,exp}$, we have from eq 1

$$\phi = U^\theta_{\phi,exp}g(R^\theta_{g,exp})\alpha_\phi(z) \tag{30}$$

which is a statement of the two-parameter theory,[13] which hypothesizes that all macroscopic properties of solutions of long chain flexible macromolecules are dependent only on two parameters, $R^\theta_{g,exp}$ and the solvent quality z. The function $\alpha_\phi(z)$ is referred to as the crossover function (or the swelling ratio) for the property ϕ due to excluded-volume effects.

For the purposes of identifying the parameters for a simulation, this equation clearly separates out HI and EV effects. While HI enters through the universal ratio under θ-conditions, the EV effect is purely determined by the parameter z. We have established elsewhere using BDS that a narrow-Gaussian potential reproduces the crossover behavior of static properties.[14] In particular, for z defined in terms of the model parameters, $z = z^*\sqrt{N}$, we have shown that the experimental data can be made to lie on simulation predictions by a suitable choice of the constant v_0. Thus, to determine the value of z under the given experimental conditions, a measurement of only a single property ϕ is required, and the corresponding theoretically predicted function $\alpha_\phi(z)$ can be used from eq 29 to perform an inversion. Therefore, on the whole, only two experimental mea-

surements are required. For example, if the radius of gyration under θ-conditions, $R^{\theta}_{g,exp}$, and at the given conditions, $R_{g,exp}$, are known, then z is uniquely given by

$$z = \alpha_g^{-1}\left(\frac{R_{g,exp}}{R^{\theta}_{g,exp}}\right) \tag{31}$$

The function $\alpha_g(z)$ is a known function of z, which can be determined by carrying out simulations as described in ref 14. Once z is known, all other properties of the system are also known and given by their corresponding functions $\alpha_\phi(z)$. Very importantly, no additional measurements are required to characterize the system. Though it would seem that z is a model parameter, it is in fact appropriate to consider it as an *macroscopic* experimental quantity (like the radius of gyration) defined by the transfer function in eq 31. We note that we have not used any model specific definitions to arrive at the above equation. Equation 31 is an experimental reality, as it is in the two-parameter theory and in the BDS results obtained here. The only difference is a single arbitrary multiplicative factor relating experimental results to either approximate two-parameter theory or to exact Brownian dynamics simulations.

As discussed in ref 14 in detail, in the case of BDS, the $\alpha_\phi(z)$ curve is obtained by keeping $z = z^*\sqrt{N}$ constant, while approaching the simultaneous limits of $N \to \infty$ and $z^* \to 0$. In this limit the parameter d^* becomes irrelevant, and as a consequence, the model predictions are insensitive to the exact value of d^* that is chosen. Further, it was shown that the corrections to the asymptotic value of α_ϕ scale as $1/\sqrt{N}$, and an extrapolation can carried be carried out similar to that for $U^{\theta}_{\phi,mod}$, discussed above. Therefore, with just two polymer specific macroscopic measurements at equilibrium, all the equilibrium predictions of the model, which are expected to be in agreement with the experimental values, are obtained when we consider a bead−spring chain model and take the limit $N \to \infty$. In particular, there is no need to fit other experimental measurements such as diffusivity, intrinsic viscosity, or the longest relaxation time to obtain the model parameters. The irrelevant parameters h^* and d^* drop out of the model and can therefore be assigned any arbitrary value for computational convenience.

3.3. Parameter-Free Predictions for a Chain of Finitely Extensible Springs at Equilibrium. As discussed previously in section 1, to accurately predict properties in nonequilibrium situations, it becomes necessary to account for the finiteness of the chain, and a commonly adopted method for doing so is to use a bead−spring chain model with finitely extensible springs (FES). It is not quite straightforward, however, to apply the equilibrium parameter estimation procedure, given above for a chain with Hookean springs, to the case of a chain with FES. A study of the long chain limiting behavior of a chain of FES, along the lines of previous works,[11,14] is necessary in order to understand the approach to universal behavior of such systems—this would then make it possible to obtain parameter-free predictions at equilibrium, or close to equilibrium, even when using a chain of FES. Though such a study is novel and important in itself, we have thought it appropriate to give the details in Appendix A to maintain continuity in our discussion of the DNA problem. Only the salient conclusions of the examination of the universal behavior of chains with FES are summarized below.

We first consider a solution under θ-conditions, modeled as an ensemble of noninteracting chains with FES. The starting point is an equation similar to eq 27, derived in Appendix A:

$$U^{\theta}_{\phi,mod}(N, h^*, b) = U^{\infty}_{\phi} + c_\phi\left(\frac{\chi(b)}{h^*} - \frac{1}{h^*_f(\chi)}\right)\frac{1}{\sqrt{N}} + \mathcal{O}\left(\frac{1}{N}\right) \tag{32}$$

While this equation is similar in form to eq 27, there are some significant differences. The first difference is the appearance of the variable χ, which is proportional to the nondimensional length of a single spring and is a function of the finite extensibility parameter b. As discussed in greater detail in Appendix A, the form of the function $\chi(b)$ depends only on the spring force model, which in the present case of DNA is a wormlike spring. The second difference is the modification of the fixed point value h^*_f, which is now a function of χ. (The dependence of the fixed point value h^*_f on χ is discussed in greater detail in Appendix A.) Recall that the parameter b depends on the number of Kuhn steps in the chain N_k and the choice of the number of beads N (see eq 24). For Hookean springs, $b \to \infty$ and $\chi \to 1$. In this limit, as we would expect, eq 32 becomes identical to eq 27. However, it can be shown that as the stiffness of the springs increases, the magnitude of b decreases and $\chi \to 0$. A value of $\chi < 1$, therefore, represents a FES with a certain degree of stiffness. In this case, both the definition of the hydrodynamic interaction parameter and the value of the fixed point are modified. It is shown in Appendix A that in the presence of FES h^* is rescaled to $\tilde{h}^*$, where

$$\tilde{h}^* = \frac{h^*}{\chi} \tag{33}$$

Consequently, the strength of HI is measured by the draining parameter $h = \tilde{h}^*\sqrt{N}$, and eq 32 can be rewritten as

$$U^{\theta}_{\phi,mod}(N, h^*, b) = U^{\infty}_{\phi} + c_\phi\left(\frac{1}{\tilde{h}^*} - \frac{1}{h^*_f(\chi)}\right)\frac{1}{\sqrt{N}} + \mathcal{O}\left(\frac{1}{N}\right) \tag{34}$$

As is evident from eq 34, the most important result of this analysis is that, even in the presence of finitely extensible springs (with a prescribed value of χ), the limiting universal ratios under θ-conditions are unaltered, i.e, $\lim_{N\to\infty} U^{\theta}_{\phi,mod}(N,h^*,b) = U^{\infty}_{\phi}$. However, the asymptotic value U^{∞}_{ϕ} is now attained in the nondraining limit, $h = \tilde{h}^*\sqrt{N} \to \infty$.

The various points discussed above are nicely illustrated by considering the universal ratio $U_{R\bar{D}}$ constructed from the Kirkwood diffusivity $\bar{\mathscr{D}}^{\theta}$ and the radius of gyration

$$U_{R\bar{D}} \equiv 6\pi\,\bar{\mathscr{D}}^{\theta}\frac{\eta_s}{kT}R^{\theta}_g = \frac{4}{\sqrt{\pi}h^*}R^{\theta *}_g\bar{\mathscr{D}}^{\theta *} \tag{35}$$

where the second equation is in terms of nondimensional model variables and $\bar{\mathscr{D}}^{\theta}$ is defined by eq 63. The approach of $U_{R\bar{D}}$ to its value in the long chain limit is

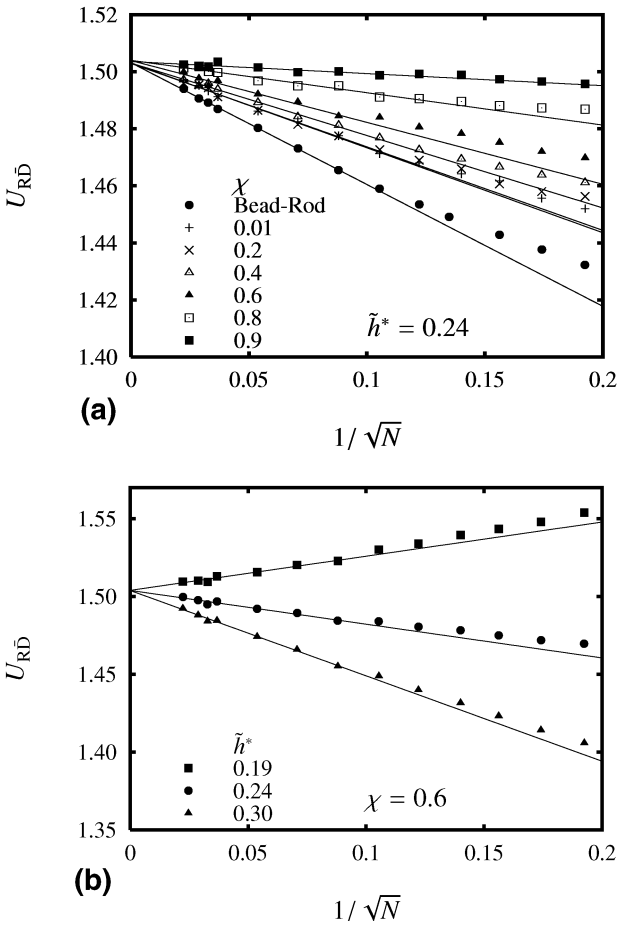

Figure 1. Scaling of the universal ratio $U_{R\bar{D}}$. Finite N data have been obtained by carrying out simulations using a FENE model. (a) The rescaled HI parameter $\tilde{h}^*$ is maintained constant in all simulations, while χ is kept constant on each trajectory. (b) The parameter χ is kept constant in all simulations, while the rescaled HI parameter $\tilde{h}^*$ is kept constant on each trajectory.

shown in Appendix A to obey the expression

$$U_{R\bar{D}} = \frac{8}{3\sqrt{\pi}} + \frac{1}{\sqrt{2\pi N}}\left(\frac{1}{\tilde{h}^*} - \frac{1}{h_f^*(\chi)}\right) + \mathcal{O}\left(\frac{1}{N}\right) \quad (36)$$

The asymptotic value is consequently $U^{\infty}_{R\bar{D}} = 8/3\sqrt{\pi} \approx 1.505$. $U_{R\bar{D}}$ can be evaluated numerically by simulating an ensemble of chains with FES at equilibrium, since the connector−vector distribution function for each spring is known from the assumed force law. We have used a simple acceptance−rejection method with a uniform distribution majorizing function to generate the chains. Results obtained by carrying out these simulations, at various constant values of χ, while keeping the rescaled parameter $\tilde{h}^*$ fixed at a value of 0.24, are displayed in Figure 1a. Symbols on each of the lines correspond to simulations carried out for a particular value of χ at various values of N. The finite chain data are then extrapolated to the limit $N \to \infty$.

It is very clear from the figure, where it can be seen that the various lines approach a common extrapolated value, that the asymptotic value of $U_{R\bar{D}}$ is independent of χ. In Figure 1b, finite chain data, accumulated for three different values of $\tilde{h}^*$, at a fixed value of χ, are shown to extrapolate to the same asymptotic value of $U^{\infty}_{R\bar{D}}$, indicating the independence of the universal ratio

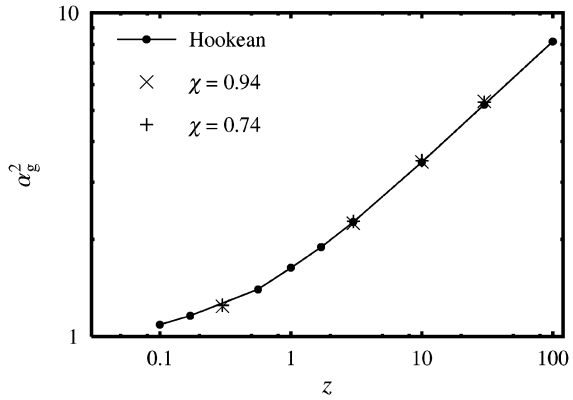

Figure 2. Swelling ratio for the radius of gyration, obtained for a chain of wormlike springs, with two different values of χ. The rescaled solvent quality parameter z is defined by eq 38. The continuous line corresponds to predictions obtained with Hookean springs.

from the particular choice made for $\tilde{h}^*$, in the nondraining limit.

It is important to bear in mind that the limit $N \to \infty$ also corresponds to the limit $N_k \to \infty$ (since χ is held constant on a trajectory). Thus, while the springs are finitely extensible, the chain itself can be considered to be infinitely long. This is because we are interested in equilibrium properties in this section, where the finiteness of the chain is not a concern. However, the equilibrium analysis has revealed what the measure of hydrodynamic interaction is in the case FES chains, and this will prove to be of some significance when we discuss the treatment of finite chains with FES (which becomes essential in the presence of flow) in the next section.

In the case of an ensemble of noninteracting FES chains in a good solvent, it is shown in Appendix A that the excluded-volume parameter z^* is rescaled to $\tilde{z}^*$, where

$$\tilde{z}^* = \frac{z^*}{\chi^3} \quad (37)$$

and the strength of excluded-volume interactions is measured by the solvent quality parameter z, given in this case by

$$z \equiv \tilde{z}^*\sqrt{N} = \frac{z^*}{\chi^3}\sqrt{N} \quad (38)$$

rather than by $z^*\sqrt{N}$. We recall that the crossover behavior in the solvent quality is obtained in the simultaneous limit of $N \to \infty$ and the interaction parameter z^* going to zero. Therefore, in the case of FES, to keep the solvent quality z at a constant value, the rescaled interaction parameter $\tilde{z}^* \to 0$ is the correct limit. The swelling ratios are then obtained at this value of z by extrapolating finite chain data to the limit of $N \to \infty$. (More details on the extrapolation procedure can be found in ref 14.) In Figure 2, the crossover function for the swelling of the radius of gyration, $\alpha_g(z)$, obtained using Hookean springs and that obtained using a chain of wormlike springs with various values of χ are shown. They can be seen to coincide with each other. This confirms that eq 38 is indeed the correct form for the solvent quality z. Further, the universal good solvent crossover behavior, when described in terms of z, remains identical to that obtained with Hookean springs

and therefore to the experiments as demonstrated in ref 14. Thus, the functions $\alpha_\phi(z)$, discussed in the previous section, are identical for FES and Hookean springs.

The essential principle underlying the existence of universal behavior at equilibrium or close to equilibrium, for chains with FES, demonstrated in Figures 1 and 2, is that when there are a large number of modes in the model, the macroscopic properties become independent of microscopic details, such as the force law.

As in the earlier discussion of HI effects, the discussion above of EV effects at equilibrium has been in the context of models where the springs have a finite length, but the properties of the chains themselves have been obtained in the long chain limit, $N \to \infty$. However, as will become clear from the discussion in the section below, the key result of this equilibrium analysis, namely, that the solvent quality is measured in terms of the variable $z = \tilde{z}^*\sqrt{N}$, will prove to be of central relevance to the treatment of EV effects in finite chains with FES.

4. Method of Successive Fine Graining (SFG)

In the presence of flow, it is clear that it in addition to using a model with finitely extensible springs the number of springs must also be finite, so that the consequences of the finite size of the molecule may be accurately represented. It is generally accepted that the most accurate representation of a linear, flexible, polymer molecule, of fixed length, is a bead−rod model with N_k rods of fixed length. However, the computational intensity of simulating bead−rod chains for the values of N_k that are typically encountered is the principal reason for the use of more coarse-grained bead−spring chain models with finitely extensible springs. As is well-known, each spring in a bead−spring model is considered to represent a set of Kuhn segments of the "underlying" polymer chain. In general, the springs in a coarse-grained FES model are chosen such that the force−extension response of a spring mimics the response of a corresponding set of segments in the underlying chain. For instance, while the FENE force law (which is actually an approximation for the inverse Langevin force law[6]) describes the force−extension behavior of a set of segments of a completely flexible chain, the WLC force law is an approximate representation of the force−extension behavior of a set of segments of a wormlike chain.

Simulations of bead−spring chain models with FES in extensional flows have shown that, in general, to predict the behavior accurately across a wide range of regimes it is necessary to use models with a large number of springs.[9] In principle, the maximum number of springs, $(N - 1)$, that one can use is equal to the number of Kuhn steps in the underlying chain. In practice, with the force models currently used, FENE or WLC, it is not possible to reach $(N - 1) \to N_k$. This is because of the limitations imposed by the nature of $\chi(b)$ in eq 24. It is straightforward to see, for instance, in the case of FENE springs, where $\chi(b) = \sqrt{b/(b+5)}$, that b becomes negative near $N = 3N_k/5$. A similar behavior can be seen in Figure 6 for the WLC force model.

The central hypothesis of the present work is that the behavior of an underlying chain with N_k Kuhn steps may be predicted by accumulating data for a bead−spring chain model with FES, at various values of N where the force law is valid, and extrapolating the accumulated results to the limit $(N - 1) \to N_k$. Since increasing values of N represent more fine-grained versions of the underlying chain, the procedure is called "successive fine graining".

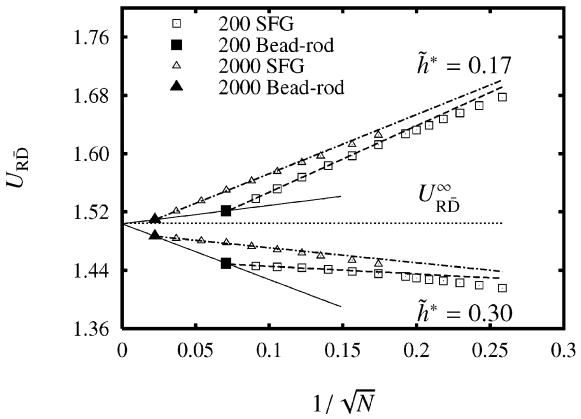

Figure 3. Illustration of the SFG procedure at equilibrium. The open symbols represent values of the nondimensional ratio $U_{R\bar{D}}$ for a FENE model, obtained at various values of N, by keeping the ratios $N_k = 200$ (square) and $N_k = 2000$ (triangle) constant. While the open symbols above the horizontal line drawn at $U_{R\bar{D}} = U^\infty_{R\bar{D}} = 1.505$ correspond to $\tilde{h}^* = 0.17$, those below the horizontal line correspond to $\tilde{h}^* = 0.30$. The filled symbols represent values obtained in the bead−rod model,[31] with the corresponding values of N_k and $\tilde{h}^*$.

For a polymer with fixed contour length (or equivalently, a fixed value of N_k), successive fine graining implies that the parameter b becomes a function of N, given by eq 24. Furthermore, during the SFG procedure, the value of $\tilde{h}^*$ is held constant as $(N - 1) \to N_k$. Physically, this is equivalent to assuming that the hydrodynamic interaction parameter at each level of the fine-graining process is constant and equal to that of the underlying chain. (Note that the conventional HI parameter $h^* = \chi \tilde{h}^*$ changes as b changes, according to eq 33.) Before discussing the treatment of solvent quality in the SFG procedure, an example of this scheme for a polymer solution at equilibrium under θ-conditions is demonstrated in Figure 3.

Figure 3 displays the dependence of the ratio $U_{R\bar{D}}$ on N, obtained by the SFG procedure, for a bead−spring chain with FENE springs, as described above. The open symbols are results of simulations carried out keeping the ratios $N_k = 200$ (squares) and $N_k = 2000$ (triangles) constant and calculating the value of $U_{R\bar{D}}$ as the chain is fine grained, at two different fixed values of $\tilde{h}^*$. Each symbol, consequently, represents a coarse-grained bead−spring chain with the same equilibrium size and contour length as an underlying bead−rod chain, with the number of rods equal to the specified value of N_k and with a hydrodynamic interaction parameter equal to the specified value of $\tilde{h}^*$. The filled symbols are exact numerical values of $U_{R\bar{D}}$ for the bead−rod model, obtained as described in ref 31. The SFG hypothesis is described by the dashed and dot−dashed curves through the open symbols, representing an extrapolation of the bead−spring chain results to the limit $(N - 1) \to N_k$. As can be seen, the extrapolated limit approaches the exact bead−rod result. It is also worthwhile to note that the bead−rod results for the different values of N_k can be extrapolated to a unique limit $U^\infty_{R\bar{D}}$, as $N_k \to \infty$, which is identical to that obtained in the previous section for chains with FES. This is in line with our expectation that universal ratios are model-independent predictions.

With regard to solvent quality, we have seen earlier in the context of chains with FES that in order to keep z at a constant value the rescaled interaction parameter, $\tilde{z}^* = z/\chi^3$, should be chosen according to $\tilde{z}^* = z/\sqrt{N}$. In the SFG procedure, this rule is applied at each level of the fine-graining process.

It is straightforward to see that the SFG procedure (i.e., $(N-1) \rightarrow N_k$), carried out for chains with finitely extensible springs, is identical in the limit of $N_k \rightarrow \infty$ to the schemes developed earlier by Kröger et al.[11] and Kumar and Prakash[14,17] for obtaining the universal behavior of models with Hookean springs, both at equilibrium and in the presence of a flow field (where the limit $N \rightarrow \infty$ is used.) For $N_k \rightarrow \infty$ and $\chi \simeq 1$ at all the levels of fine graining which are accessible computationally, and as a result, $\tilde{h}^* \simeq h^*$ and $\tilde{z}^* \simeq z^*$. Indeed, the universal behavior that was observed for models with Hookean springs, with results independent of the choice of both h^* and d^*, was a consequence of the infinite length of the chain. For chains with finite values of N_k, the SFG procedure implies that in the limit $(N-1) \rightarrow N_k$ the draining parameter has a finite value $h = \tilde{h}^*\sqrt{N_k}$ and $\tilde{z}^* = z/\sqrt{N_k} \neq 0$. For instance, for λ-phage DNA, with an estimated value of $N_k = 200$ (as discussed in greater detail subsequently), a choice of $\tilde{h}^* = 0.2$ leads to $h \simeq 3$. We might anticipate therefore that, in this case, the extrapolated results might not be universal, since the nondraining limit may not be attained, and there might even be a dependence on the choice of d^*. The existence of universal behavior clearly depends quite crucially on the value of N_k and on the interaction of the flow with the polymer, determined by the magnitudes of the Weissenberg number Wi and the Hencky strain ϵ.

In the next section, we carefully examine this question, using all the procedures that have been described so far. First, universal results in extensional flow are obtained for bead−spring chain models with Hookean springs, both at θ-conditions and under good-solvent conditions. Since such models correspond to infinitely long polymers, they do not exhibit a coil−stretch transition, and model predictions grow without bound with increasing values of strain. Nevertheless, as will be clear from the discussion below, they serve as a basis with which the behavior of finite chains may be compared.

5. Universality and Finite Size Effects

In the experiments reported in ref 3, λ-DNA was subjected to a sudden elongational flow starting from an equilibrated state and observed under a microscope as it evolved from a coillike state to the fully stretched state, at various elongational rates. The size of a fluorescently dyed DNA coil, measured by this method, is a projected extent in the flow direction, commonly called the "extension" or "stretch". In terms of a bead−spring model this is defined as $x_{max} \equiv \max_{\mu,\nu}|r_\mu^x - r_\nu^x|$, where r_μ^x is the x-component of vector $\mathbf{r}_\mu$, with x being the flow direction. The statistical properties of this quantity, unlike R_g or end-to-end distance, are not easy to calculate analytically.[5] On the other hand, since it is straightforward to evaluate the stretch from a given configuration of bead positions, a knowledge of the distribution function obeyed by the configurations implies that the average stretch can be obtained numerically from an ensemble of configurations. Here, the average along the direction of intended elongation is denoted as $\bar{x} \equiv \langle x_{max} \rangle$. In particular, while the equilibrium stretch is denoted by $\bar{x}$, the stretch at any nonzero finite value of the strain is denoted by $\bar{x}^+$, in keeping with the accepted rheological convention for transient properties. It is worthwhile to note that at equilibrium the average stretch of a long flexible chain is not equal to exactly twice the radius of gyration R_g, as assumed in ref 3. For instance, in the limit of long chains obeying a Gaussian distribution (θ-conditions), we can numerically evaluate this to be

$$\frac{\bar{x}^\theta}{2R_g^\theta} = 1.132 \pm 0.001 \tag{39}$$

In the first part of this section, the universal stretch experienced by a polymer chain in uniaxial extensional flow is predicted by examining the behavior of a bead−spring chain model, with Hookean springs, in the long chain limit. While experimental data on the stretch are typically reported in terms of the nondimensional ratio $\bar{x}^+/L$, where L is the contour length of the DNA molecule, this is clearly not usable in the case of Hookean springs, where $L \rightarrow \infty$. Consequently, universal behavior is examined here in terms of the expansion factor E, defined by

$$E = \frac{\bar{x}^+}{\bar{x}} \tag{40}$$

which is the ratio of the transient stretch at a given solvent quality to its value at equilibrium at the same solvent quality. This ratio has the correct scaling behavior for Hookean spring chains in the limit $N \rightarrow \infty$.

As mentioned earlier, a crucial parameter that arises in flow is the Weissenberg number, Wi. In this work, it is taken to be the same as defined in experiments of Smith and Chu,[3] namely

$$Wi = \dot{\epsilon}\lambda_1 \tag{41}$$

where λ_1 is the longest relaxation time. Smith and Chu evaluated this characteristic time constant by fitting an exponential to the tail end of the relaxation of the function $\bar{x}^2(t)$, where $\bar{x}(t)$ is the average instantaneous stretch, when a fully stretched DNA is left to relax to equilibrium. We have employed a similar procedure to determine the longest relaxation time, as described in greater detail below.

It has been established in section 3.2 that macroscopic predictions of bead−spring chains with Hookean springs, in the limit $N \rightarrow \infty$, do not depend on the microscopic parameters of the model, h^*, z^*, and, d^*. However, since the simulations are carried out with finite N, it is necessary to assign values to these variables, consistent with known equilibrium data, but arbitrarily chosen for computational convenience. The stepwise procedure for parameter determination is outlined below.

1. The number of beads N: An arbitrary number of beads N is chosen, and all the following parameters are dependent on this choice of N.

2. The interaction parameters for HI (h^*) and EV (z^*, d^*): Since any arbitrary value of h^* can be chosen, we have chosen $h^* = 0.19$ and 0.3, which bracket the fixed point value, $h_f^* = 0.24$ (with preaveraged HI). Note that for Hookean springs, as mentioned earlier, $\tilde{h}^* = h^*$, since $\chi = 1$.

For a given value of the solvent quality z, the EV parameters used in the narrow-Gaussian potential are

determined from

$$z^* = \frac{z}{\sqrt{N}} \tag{42}$$

$$d^* = Kz^{*1/5} \tag{43}$$

where K is an arbitrary constant. Clearly, for a fixed value of z, since $z^* \to 0$ as $N \to \infty$, this choice of d^* implies that the asymptotic limit is reached along trajectories in the (z^*, d^*) parameter space that converge to the origin. Kumar and Prakash[14,17] have shown previously that the asymptotic results are independent of the particular choice of K and that choosing d^* values according to eq 43 permits the use of larger step sizes in the numerical integration scheme.

3. The relaxation time λ_1^*: Under good solvent conditions, the longest relaxation time is obtained here by fitting a single exponential to the decay of three different size measures: (a) the mean-square end-to-end distance, (b) the mean-square radius of gyration, and (c) the mean-square stretch, after initially extending a chain by stretching each spring in the chain to roughly twice its equilibrium length. The curve is fitted using

$$s^* = s_\infty^* + (s_0^* - s_\infty^*)\mathrm{e}^{-t^*/\lambda_1^*} \tag{44}$$

to determine the three parameters λ_1^*, s_0^*, and s_∞^*, where s^* is one of the variables listed above. The range of the fit was adjusted over 2 decades in the variable $(s^* - s_\infty^*)/s_\infty^*$ starting from a value of 1. The difference in the relaxation times for a given N, obtained from the decay of the three different size measures listed above, was found to be within 3%.

Under θ-conditions, the well-known Thurston's expression,[6] which predicts the longest relaxation time for any given choice of h^* and N, has been used. It was found, by rigorous comparison for a few cases with the exponential curve-fitting procedure described above, that Thurston's expression was valid within about 6%.

4. Elongation rate $\dot{\epsilon}^*$: The experiments were performed at various Weissenberg numbers Wi, ranging from 2 to 55. The nondimensional elongational rate required for the simulations is given by $\dot{\epsilon}^* = Wi/\lambda_1^*$.

Once data are accumulated for various finite values of chain length N, it can be extrapolated to the long chain limit. In Figure 4, the expansion factor E, obtained by following the procedure above, is plotted against $1/\sqrt{N}$, at a constant strain $\epsilon = 4$ and constant Weissenberg number $Wi = 2$ for various cases. In Figure 4a,b, the HI parameter, $\tilde{h}^* = h^*$, is held constant at two different values during the fine-graining procedure, while in Figure 4c, the parameter K is held constant at two arbitrarily chosen values. Figure 4a corresponds to a θ-solution, while Figure 4b,c corresponds to the case of a good solvent with $z = 1$. The independence of the extrapolated result in the long chain limit, in each of these cases, from the particular choice made for these parameter values, is clearly seen in these figures. As a result, the asymptotic value of E, obtained in this manner, is the universal value of this property at $\epsilon = 4$ and $Wi = 2$.

By carrying out an extrapolation procedure, similar to that displayed in Figure 4, at various values of the Hencky strain, the universal transient stretch experienced by an infinitely long polymer chain, in the nondraining limit, may be predicted. Figure 5 displays

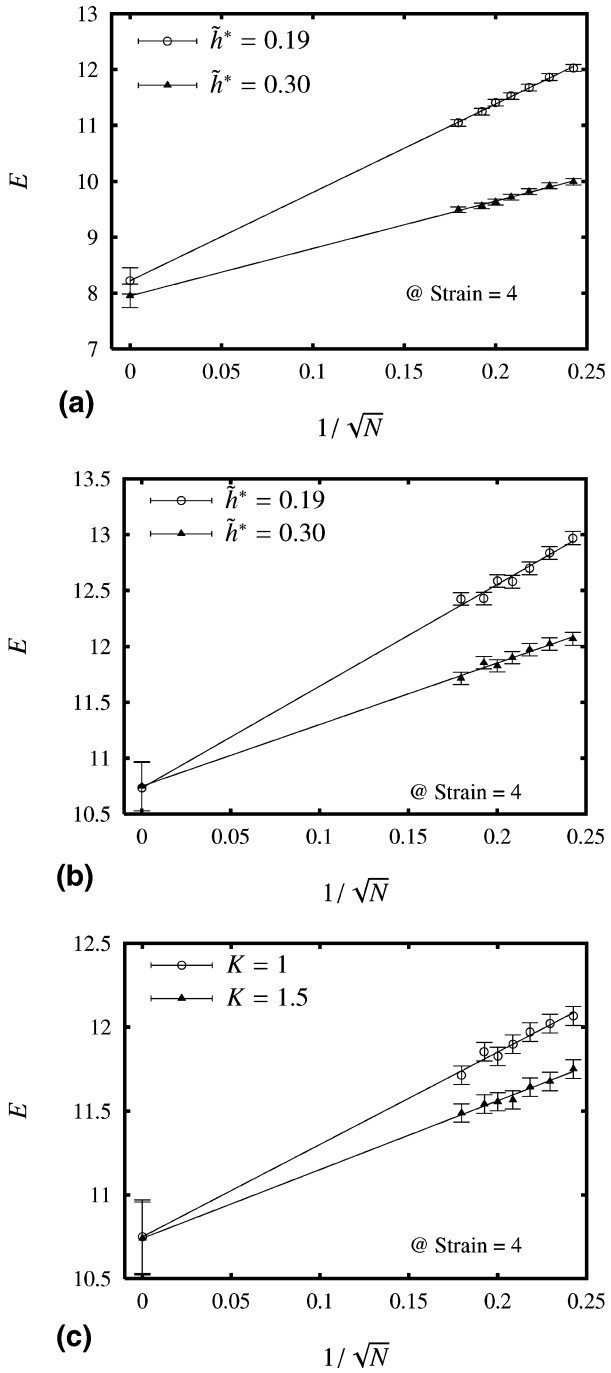

Figure 4. Independence of the asymptotic value of the expansion factor, E, from the choice of h^* and d^*, at Hencky strain $\epsilon = 4$ and Weissenberg number $Wi = 2$. (a) θ-conditions, effect of $\tilde{h}^*$, (b) $z = 1$, effect of $\tilde{h}^*$ with $K = 1$, and (c) $z = 1$, effect of d^* with $\tilde{h}^* = 0.3$. d^* is varied according to eq 43, with two different values of K.

the results of such an exercise, for $Wi = 2$, under both θ-conditions and for a good solvent with $z = 1$.

As is expected for a bead−spring chain model with Hookean springs, the curves increase without bound for increasing values of ϵ. As a result, the stretch never reaches a steady-state value. Physically, the infinite polymer coil is being unravelled continuously but never undergoes a coil−stretch transition because of the existence of infinite length scales. The role played by the presence of excluded-volume interactions is also clearly discernible—the initially expanded coil structure is unravelled more rapidly by the flow. The influence

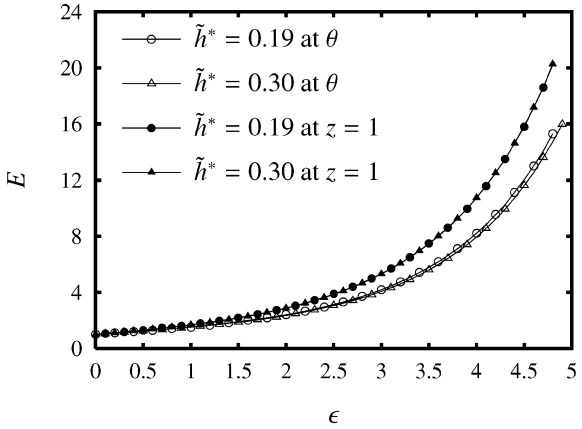

Figure 5. Universal behavior in extensional flow. Expansion factor E as a function of Hencky strain, at $Wi = 2$, under θ-conditions and at $z = 1$, obtained using Hookean springs in the limit $N \rightarrow \infty$.

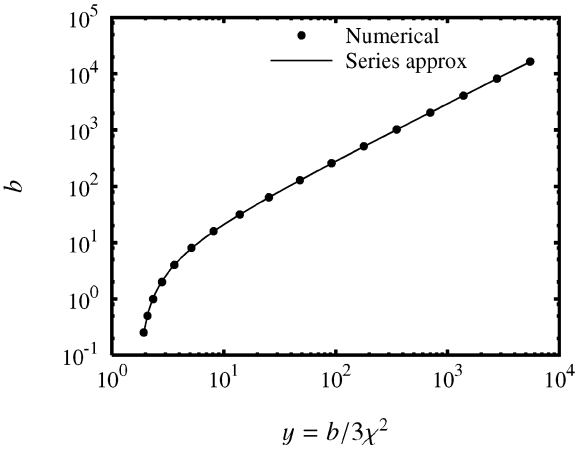

Figure 6. Determination of the parameter b for a wormlike spring, for given values of N and N_k, using the series approximation, eq 46.

of EV effects in infinite chains, relative to its influence in finite chains, is considered in greater detail later in this section (see discussion related to Figure 11).

While the data for the two values of $\tilde{h}^*$, at $z = 1$, are superimposed on each other for all the strain values displayed in Figure 5, the data at high values of strain, under θ-conditions, appear to be coming apart. This merely indicates that the presently accumulated finite chain data are not adequate to obtain accurate and unique extrapolated values (as seen, for instance, in Figures 4a) at these values of strain. However, in principle, this is easily remedied by carrying out similar simulations at even larger values of N.

It is worthwhile to note that the results displayed in Figure 5 are *exact* universal predictions, with fluctuating hydrodynamic and excluded-volume interactions, obtained here for the first time by exploiting the extrapolation ansatz for Hookean springs developed by Kröger et al.[11] and Kumar and Prakash.[14]

We turn now to predictions of the expansion factor E, for a chain of finite length, using the method of successive fine graining, outlined in section 4. As pointed out in that section, the two key differences from the case of a chain with infinite length considered above are the use of finitely extensible springs and the restriction of the extrapolation process to the limit $(N - 1) \rightarrow N_k$. These differences imply a change in some of the steps of the finite chain parameter determination procedure, described above for Hookean springs. Basically, an additional parameter b is introduced through the use of FES, with the concomitant appearance of the function χ and the need to rescale the HI and EV interaction parameters. For the sake of clarity, the steps that are changed are enumerated below.

1. The finite extensibility parameter b: For given values of N_k and N, the corresponding value of b can be found by solving the nonlinear expression, eq 24. The solution is not available in closed form for a wormlike-spring force law, since $\chi(b)$ itself has to be evaluated numerically, as given in Appendix B. However, an approximate procedure can be developed which yields the value b to a high degree of accuracy. First, note that the function $y(N) \equiv b/3\chi^2(b)$ can be readily evaluated given N_k and N, since from eqs 24

$$y(N) = N_k \frac{N+1}{N(N-1)} \tag{45}$$

By numerically evaluating $\chi(b)$ for various values of b, the relationship between b and y can be obtained for a given force law and plotted once and for all, as shown for WLC springs in Figure 6. As a result, the value of b, corresponding to given values of N_k and N (and, therefore, y), can be simply read off from the figure. It turns out that this procedure can be further simplified since it was found that the numerical data could be described very accurately with the following series representation

$$b = 3y\left[1 + \frac{c_1}{\sqrt{y}} + \frac{c_2}{y} + \frac{c_3}{y^2} + \frac{c_4}{y^3}\right] \tag{46}$$

where the parameters $c_1 = -0.63$, $c_2 = -1.0$, $c_3 = -0.70$, and $c_4 = 1.47$ have been obtained by a systematic nonlinear least-squares regression fit of the numerical data in the b vs $b/3\chi^2$ space. Thus, using the value of y, b is determined from eq 44. Subsequently, $\chi(b)$ can be obtained, as given in Appendix B. Note that the series has the correct asymptotic form for $y \rightarrow \infty$, corresponding to the Hookean limit. The accuracy of the approximation is evident from Figure 6, where it can be seen that values obtained from the series representation virtually coincide with the numerical data. We have taken $N_k = 200$ in the calculations to follow.

2. The rescaled interaction parameters for HI (h^*) and EV (z^*, d^*): As described in section 4, any arbitrary value of $\tilde{h}^*$ can be chosen. The corresponding value of h^* is determined from $h^* = \chi(b)\tilde{h}^*$. We have chosen the values $\tilde{h}^* = 0.19$ and 0.3 to carry out comparisons with the results obtained earlier for Hookean springs. For a given value of the solvent quality z, the strength of the excluded-volume interaction, at each level of the fine-graining process, is determined from $z^* = \chi^3(b)z/\sqrt{N}$, while d^* is obtained from eq 43, as in the case of Hookean springs.

3. The reference scales l_H and λ_H: In a situation where it is desired to compare the model predictions to a dimensional experimental measurement, it is necessary to obtain the values of the reference scales of length l_H and time λ_H at any given level of discretization, N. As described in section 3.1, l_H can be found from eqs 16 and 23, while λ_H can be obtained from eq 18.

4. The relaxation time λ_1^*: The procedure for determining the relaxation time is identical to the case of Hookean springs, with the minor difference that the

Table 1. Typical Parameter Values Encountered in the Successive Fine-Graining Procedure for a Wormlike Chain with $N_k = 200$, $L = 22\ \mu m$, $z = 1$, $\eta_s = 43.3$ cP, $T = 296$ K, $\tilde{h}^* = 0.19$, and $K = 1$

N	b	$\chi(b)$	$l_H(\times 10^{-5}$ cm)	λ_H(s)	λ_1^*
11	54.00	0.910	2.99	0.41	16.5 ± 0.1
19	25.71	0.858	2.41	0.20	36.5 ± 0.4
27	15.56	0.808	2.14	0.13	60.0 ± 0.5

stretch relaxation was carried out after first extending chains to 85% of their maximum length.

Table 1 lists the key parameter values and the resultant nondimensional relaxation time λ_1^*, obtained by the above procedure, at various levels of discretization, as an illustration of typical magnitudes encountered in the simulations. It is important to note here that for a given vale of N the nondimensional relaxation time is relatively insensitive to the value of N_k when it was chosen in the range 150−300. This will prove to be a crucial point when comparisons are made with experimental observations on DNA in section 6. As will be discussed in greater detail below, it was found that for λ-DNA a maximum of $N = 33$ was sufficient to obtain reliable extrapolations of the average stretch evolution in elongational flow in the limit $(N - 1) \to N_k$. The SFG procedure is tedious to some extent since for each value of N, we need to first determine the corresponding λ_1^*, as given in Table 1. Note, however, that for a given value of N the choice of $\tilde{h}^*$ and the d^* is still arbitrary. We have used 10^4 polymer chains in an equilibrium ensemble to determine the relaxation time and about 10^5 polymer chains for a nonequilibrium simulation.

Values of the expansion factor E, for various values of $1/\sqrt{N}$, obtained for a model with WLC springs, using $N_k = 200$, and two different values of $\tilde{h}^*$, at fixed values of $\epsilon = 4$ and $z = 1$ (with the parameter values for different choices of N determined as described above), are displayed in Figure 7. While Figure 7a corresponds to the Weissenberg number $Wi = 2$, Figure 7b corresponds to $Wi = 55$. The lines through the symbols represent extrapolations of the finite chain data to the limit $(N - 1) \to N_k$. It is clear from Figure 7a that at $Wi = 2$ the extrapolated values at $N = N_k$ are insensitive to the choice of $\tilde{h}^*$. On the other hand, at a high Weissenberg number, such as $Wi = 55$, the extrapolated values for the two different values of $\tilde{h}^*$ are distinct. This is clearly dependent on the value of strain, as can be seen from Figure 8, where the results of carrying out a similar extrapolation procedure, at various values of the Hencky strain, are displayed.

At the relatively low value of Weissenberg number, $Wi = 2$, the expansion factor is clearly insensitive to the choice of $\tilde{h}^*$ at all values of the strain. On the other hand, at $Wi = 55$, the different values chosen for $\tilde{h}^*$ get "revealed" as the strain increases. This is entirely consistent with our previous discussion, where it was argued that the coillike structure of the chain at equilibrium, and close to equilibrium, masks the local details of the chain (such as the nondimensional bead radius) from the flow, while at higher Weissenberg numbers, and large values of strain, the polymer chain is exposed to the flow field as it unravels to a stretched state. In the case of bead−spring chain models with FENE springs, the SFG procedure reveals a similar insensitivity to the value of $\tilde{h}^*$ at all values of the strain for $Wi = 2$, while a slight separation of the curves for large values of strain occurs at $Wi = 55$ (see also Figure 10).

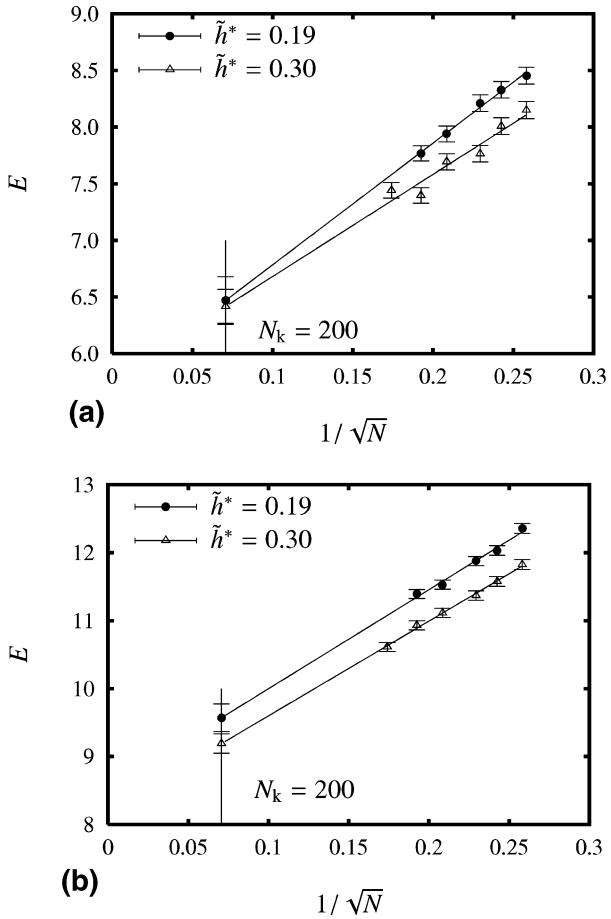

Figure 7. Illustration of the SFG procedure for a model with WLC springs, at a fixed value of Hencky strain, $\epsilon = 4$ and at Weissenberg numbers (a) $Wi = 2$ and (b) $Wi = 5$. Parameter values are $N_k = 200$, $z = 1$, and $K = 1$. Symbols for $N < N_k$ have been obtained by carrying out simulations at two different values of $\tilde{h}^*$. Lines through the symbols represent an extrapolation to the limit $(N - 1) \to N_k$.

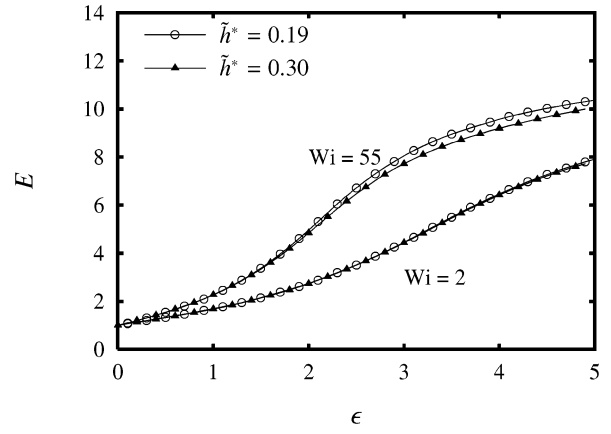

Figure 8. Expansion factor E, in extensional flow, for a model with WLC springs at two different Weissenberg numbers and two different values of $\tilde{h}^*$. Symbols are extrapolated values, obtained by the SFG procedure. Parameter values are the same as in Figure 7.

In Figure 4c, the independence of the infinite chain length results, from the value chosen for the narrow-Gaussian potential parameter, K, was clearly demonstrated. As discussed earlier, when eq 41 is used, $d^* \to 0$ as $N \to \infty$ for fixed values of z. Since the parameter d^* represents the range of excluded-volume interactions between the beads, this limit clearly corresponds to a

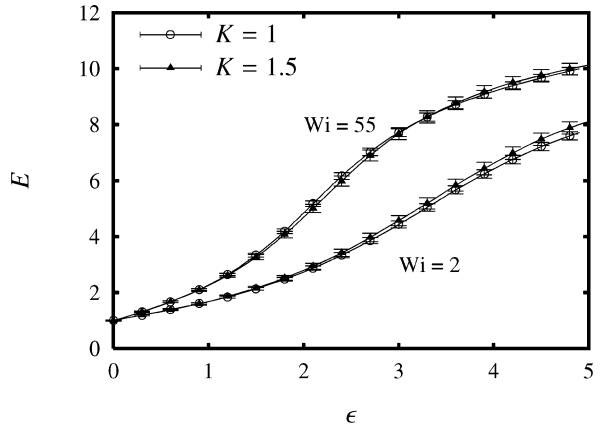

Figure 9. Sensitivity of the expansion factor to the range of excluded-volume interactions. Symbols are extrapolated values for two different values of K, obtained by the SFG procedure. Parameter values are $N_k = 200$, $\tilde{h}^* = 0.19$, and $z = 1$.

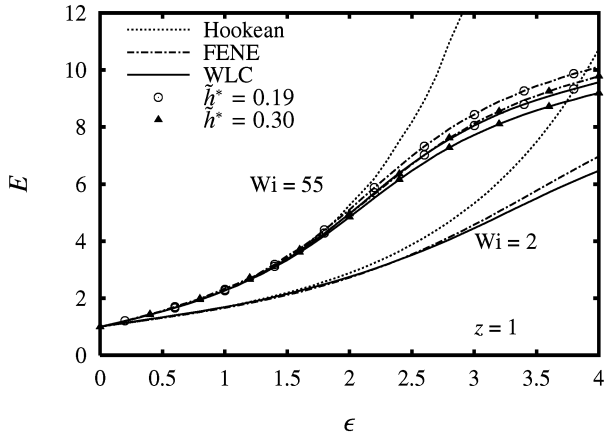

Figure 10. Expansion factor for Hookean, WLC, and FENE force laws, at two different Weissenberg numbers and two different values of $\tilde{h}^*$, obtained by the SFG procedure. At $Wi = 2$, data for the two values of $\tilde{h}^*$ agree to within simulation error bars (see also Figure 8). Parameter values are the same as in Figure 7.

δ-function excluded-volume potential. In the case of finite chains, however, we have seen earlier that the limit $(N-1) \to N_k$ implies $\tilde{z}^* = z/\sqrt{N_k} \neq 0$. As a result, different choices for the parameter K imply different limiting values for the range of excluded-volume interactions.

In Figure 9, the expansion factor for two different values of K, at $Wi = 2$ and $Wi = 55$, obtained with the SFG procedure for a chain with WLC springs, is displayed. Differences between the extrapolated predictions for the two values of K lie within the error bars of the simulations, indicating the relative insensitivity of the expansion factor to this parameter. Since, for $Wi = 2$, we have previously observed the independence of the expansion factor from the particular choice of $\tilde{h}^*$, the displayed curve for $Wi = 2$ in Figure 9 is in some sense "parameter-free" and dependent only on the number of Kuhn steps in the chain and the spring force law.

In both Figures 8 and 9, the expansion factor at large strains is seen to level off to an asymptotic steady state value, clearly highlighting the central difference between finite and infinite chains. At a threshold value of strain that depends on the Weissenberg number, the finite character of the chain leads to the existence of a point of inflection on the curves, where the slope stops increasing and starts to decrease. Since the finiteness of the chains is incorporated in the model by the use of finitely extensible springs, it may be anticipated that nature of the deviation of the finite chain curves, from the universal Hookean curve, depends on the choice of the spring force law.

Differences in predictions by the various force laws are highlighted in Figure 10, where the expansion factor obtained with Hookean, WLC, and FENE force laws, using the SFG procedure, at two different Weissenberg numbers and two different values of $\tilde{h}^*$, are compared. While the expansion factor predicted by the Hookean force law is unbounded, the incorporation of FES ensures a bounded value of the expansion factor at high values of the strain. The expansion factor predicted by all three force laws is identical at small values of strain. However, at a value of strain $\epsilon \simeq 1.5$, the FES force law predictions depart from the Hookean predictions. The agreement at low values of strain is not surprising since the polymer chain is predominantly in the coiled state. In this case, as we have seen earlier, results become relatively independent of local details such as the spring force laws. For $Wi = 2$, both the WLC and the FENE force law predictions are identical until $\epsilon \simeq 2.5$, beyond which a difference in the predictions can be discerned. Interestingly, at $Wi = 55$, the separation of the curves for the two values of $\tilde{h}^*$, and the separation of the FES curves from the Hookean curves, occur at roughly the same value of strain, $\epsilon \simeq 1.5$. (It is perhaps appropriate here to note that maintaining a constant value of $\tilde{h}^*$ for both the WLC and FENE models actually implies using different values of h^* at each stage of the fine-graining process, since the function $\chi(b)$ is different for the two force laws.)

It is clear from Figure 10 that the universal (Hookean) stretch vs strain curve acts as an envelope for all possible finite chain, stretch vs strain, curves. Essentially, for a given value of the Weissenberg number, the strain at which a finite chain curve departs from the Hookean curve, would depend on the value of N_k. For increasing values of N_k, the point of departure would occur at increasing values of strain.

The role of excluded-volume interactions in models with Hookean springs was elucidated earlier in Figure 5. Before we examine their role in models with FES, it is necessary to introduce some new notation. Consistent with the definition of equilibrium swelling ratios, the swelling of the equilibrium stretch is denoted by

$$\alpha_x = \frac{\bar{x}}{\bar{x}^\theta} \tag{47}$$

In a transient extensional flow, we introduce the transient swelling ratio α_x^+ to represent the ratio of the stretch in extensional flow under good solvent conditions to its value under θ-conditions, evaluated at the same value of strain:

$$\alpha_x^+ = \frac{\bar{x}^+}{\bar{x}^{+\theta}} \tag{48}$$

The relationship between the transient swelling ratio α_x^+ and the expansion factor E defined earlier can be derived from

$$\alpha_x^+ = \frac{\bar{x}^+}{\bar{x}} \frac{\bar{x}^\theta}{\bar{x}^{+\theta}} \frac{\bar{x}}{\bar{x}^\theta} \tag{49}$$

$$\alpha_x^+ = \frac{E}{E_\theta}\,\alpha_x \tag{50}$$

where $E_\theta = \bar{x}^{+\theta}/\bar{x}^\theta$. Note that the equilibrium expansion factor depends on z through its crossover function, $\alpha_x = \alpha_x(z)$.

In Figure 11, the dependences of α_x^+ on strain, for models with Hookean springs and WLC springs, are compared. The data for Hookean springs can be obtained from that displayed earlier in Figure 5 and eq 50. The curves for WLC springs have been obtained in a similar manner by applying the SFG procedure. It is clear that α_x^+ for Hookean springs continues to increase with increasing strain, indicating that excluded-volume interactions are always present. This is a consequence of the fact that the chain is infinitely long, and at any value of flow strength, there are always length scales at which beads exclude each other. On the other hand, in the case of FES chains, once the coil becomes stretched, the excluded-volume interactions get switched off as the beads are drawn increasingly further apart. Though at equilibrium ($\epsilon = 0$) the swelling of a chain with $z = 3$ is greater than that with $z = 1$, α_x^+ decreases in both cases ultimately to a common steady-state value—albeit after an initial range of strain values in which it increases slightly.

It would be worthwhile to confirm these predictions with careful experimental investigations. At the moment, the available experimental data on λ-phage DNA are insufficient to enable a precise estimation of the solvent quality, as will be seen from the detailed discussion below. However, we can obtain a reasonable validation of the ideas presented so far by comparing the predictions of the present simulations, obtained with the SFG procedure, with the experimental data of Smith and Chu.[3]

6. Application of SFG to DNA

Before we use the method of successive fine graining, we first justify applying the general approach for modeling flexible macromolecules to λ-DNA. DNA is a polyelectrolyte, and when in solution the electrostatic effects can lead to spatially long-range interactions. This precludes the use of the scaling arguments used for flexible macromolecules. In the presence of excess salt, however, the electrostatic interactions become screened[32] and become local (the range of interactions falling below the persistence length of the chain) and can in effect be treated as an excluded-volume interaction between distant portions of the chain, similar to the excluded-volume effects seen in good solvents. It is reasonable, therefore, to accord DNA a treatment similar to a flexible molecule in a good solvent.

6.1. Estimation of Parameters for λ-DNA at Equilibrium. As discussed in the previous section, to capture the behavior of a finite-length polymer molecule under flow, we require, in the successive fine-graining method, only three equilibrium properties of the polymer, namely, the radius of gyration under θ-conditions R_g^θ, the solvent quality z, and the contour length L. Further, when we are interested in making nondimensional predictions shown in the previous section, only the number of Kuhn steps N_k (which is related to ratio of L to R_g^θ through eq 24) and z are required.

In the context of estimating these parameters for the purpose of comparing predictions with the experimental

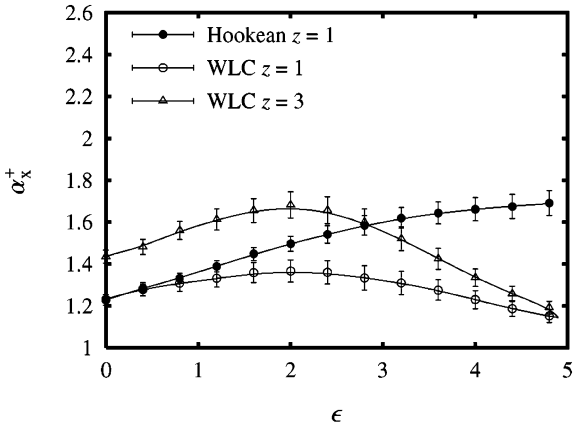

Figure 11. Dependence of the transient swelling ratio on the strain and solvent quality, for models with Hookean springs (filled circles) and WLC springs (open symbols). For the latter, $N_k = 200$. In both cases, $Wi = 2$. Hookean results have been obtained in the limit $N \to \infty$, while WLC results have been obtained by the SFG procedure. At this value of Wi, the latter are independent of the choice of K and $\tilde{h}^*$.

observations of Smith and Chu,[3] there are certain issues that need to be addressed with regard to the particular experimental systems considered in their work. The contour length for YOYO-1 stained λ-DNA is known to be $L \simeq 22\ \mu$m.[3] To the best of our knowledge, a direct measurement of the radius of gyration of λ-DNA under the given solvent conditions considered has not been reported. Additionally, various experimental quantities required for the elongational flow experiment were obtained in different solvent media (the buffer solution was changed to alter the viscosity), and this could be responsible for changes in solvent quality. For instance, the diffusivity was measured in a 0.95 cP solvent,[2] and the longest relaxation time was determined in a 41 cP solvent,[33] while the elongational flow experiments were performed in solvent viscosities ranging from 43.3 to about 180 cP[3] to obtain a control on the strain rate relative to the longest relaxation time of the molecule. Therefore, it is difficult to ascertain the two parameters R_g^θ (or N_k) and z accurately.

An estimate of N_k can be obtained from the force extension curves,[34] which suggest a persistence length $\lambda_p = 66$ nm for YOYO stained DNA.[35] From this we have $N_k = L/(2\lambda_p) \approx 167$ or equivalently $R_g^\theta = 0.69\ \mu$m. While this interpretation is widely used, there is also an alternative suggestion, based on other experiments, that the persistence length is much lower[36]—around $\lambda_p \sim 28.5$ nm at high salt concentrations, which corresponds to ~38 nm for stained DNA. This would then imply $N_k \sim 289$ and $R_g^\theta = 0.53\ \mu$m.

It is also possible, in principle, to obtain an estimate for N_k and z using other measurements of λ-DNA, which are consistent with the universal behavior discussed in section 1. For instance, the equilibrium stretch, diffusivity, and relaxation time can be used to construct universal ratios, from which R_g^θ and z can be estimated using the universal crossover behavior. However, such an attempt is presently infeasible for two reasons: (i) an absence of careful studies of the swelling ratios for DNA under various solvent conditions, to ensure that DNA solutions exhibit universal behavior, and (ii) the presence of a large uncertainty in the measured stretch of λ-DNA close to equilibrium. (It has been reported that the observed coil size is exaggerated due to a "blooming effect" in the video camera, and a constant factor of 1

μm has been suggested as the offset correction to be subtracted from the observed size. The magnitude of the suggested correction is based on an approximate estimate of the actual equilibrium stretch, obtained from a knowledge of the radius of gyration. However, the radius of gyration is in turn only calculated from the Zimm model under good-solvent conditions, using diffusivity measurements.[2])

It is clear, therefore, that there are several uncertainties in assigning values to R_g^θ and z. The main emphasis in the present paper, however, is on developing an appropriate framework for the treatment of solvent quality effects, under nonequilibrium conditions. It is consequently perhaps not so crucial that at present it is not possible to obtain accurate estimates of these quantities.

The arguments above suggest estimates of N_k in the range 166−289. To make comparisons with the experiments, this does not pose a serious problem if we represent all the quantities in a nondimensional form. This is because (a) the relaxation times λ_1^* are insensitive to the value of N_k in the range 150−300 (see section 5) and (b) extrapolated values of E are indistinguishable within error bars when $(N-1) \to N_k$, for values of N_k in this range (as can be seen in Figure 7). Therefore, for the purpose of comparing with experimental observations below, we take $N_k = 200$ as a representative value.

A similar argument cannot, however, be made for the solvent quality, as its effect in elongational flow is clearly evident from Figure 11. In the absence of accurate estimates, we assume $z = 1$. In combination with $N_k = 200$, as will be seen shortly below, this value of z leads to reasonably accurate estimates of both the equilibrium stretch and the stretch during extension.

With $N_k = 200$ and $L = 22$ μm, we can compute $R_g^\theta = 0.63$ μm using eq 25 and $\bar{x}^\theta = 1.43$ μm using eq 39. We have determined the universal crossover of the swelling of the equilibrium stretch and found that at $z = 1$, $\alpha_x = 1.25$. This gives the equilibrium stretch in good-solvent conditions to be $\bar{x} = 1.79$ μm. The measured stretch (extension) in Figure 2A in ref 3, when extrapolated to zero strain, is 2.55 ± 0.02 μm. The difference of $\sim$0.8 μm can therefore be attributed to blooming. It should be noted that the available data have been used only to obtain a rough estimate of the various parameters, and in the light of more accurate measurements in the future, some of these calculations would need to be repeated.

6.2. DNA in Elongational Flow. With the specification of R_g^θ, z, and the contour length, the equilibrium specifications required to carry out the successive fine graining is complete. The only other relevant parameter entering the flow situations is the Weissenberg number Wi. We use the same definition of Wi (or the Deborah number De) as considered in ref 3: $Wi = \dot{\epsilon}\lambda_1$. In all the simulation results discussed in this work, we consider two cases, namely, the smallest and largest Wi reported in ref 3, $Wi = 2$ and 55, to explore model predictions.

First, we superimpose the results displayed earlier in Figure 10, which has been computed with $N_k = 200$ and $z = 1$, on the experimental observations of stretch vs strain, as shown in Figure 12. For the experiments, we have subtracted a blooming correction of 0.8 μm, found above, from the measured stretch uniformly at all strains, and divided it by the stretch at zero strain. Figure 12 clearly shows the universal nature of the unravelling of λ-DNA (when compared with Hookean curve), up to about strains $\simeq 2$ units, after which finite size effects begin to play a role. As we know from the discussions in the earlier sections, the existence of universality implies that the expansion factor E is independent of the parameters $\tilde{h}^*$ and d^* and depends only on the solvent quality z.

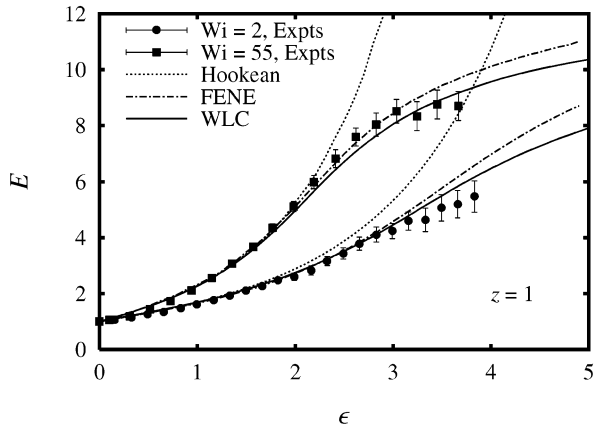

Figure 12. Comparison of the expansion factor predicted for Hookean, WLC, and FENE force laws, at two different Weissenberg numbers, with the experimental observations of Simth and Chu.[3] Parameter values are the same as in Figure 7.

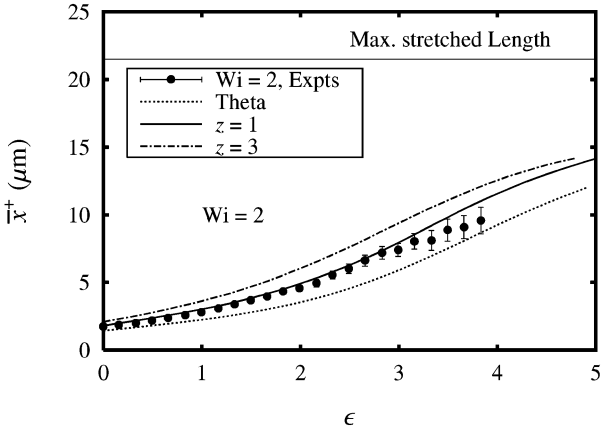

Figure 13. Effect of solvent quality on the absolute stretch of λ-DNA in elongational flow. Theoretical predictions under θ-conditions and two different solvent qualities, $z = 1$ and $z = 3$, are compared with the experimental results of Smith and Chu.[3] The maximum contour length of the chain, $L = 22$ μm, is also displayed. Parameter values are $N_k = 200$, $\tilde{h}^* = 0.19$, and $Wi = 2$.

At values of strains beyond $\epsilon = 2$, Figure 12 shows that, within experimental errors, (a) the curves agree with experiments, for the values chosen for $\tilde{h}^*$ in Figure 10, namely, $\tilde{h}^* = 0.19$ and $\tilde{h}^* = 0.3$, and (b) both the FENE and WLC model predictions (for these values of $\tilde{h}^*$) agree with the experimental measurements. Clearly, only data obtained at higher strains and more accurate measurements can resolve the differences seen in the theory.

In Figure 13, we examine the effect of solvent quality using only the WLC force model for the springs. Here we choose to compare the absolute values of the stretch $\bar{x}$ instead of using the expansion ratio E. Ideally, a comparison of the transient swelling ratio (displayed in Figure 11), with experimental observations, would have clearly revealed the differences that solvent quality can induce in the unravelling rate. In the absence of such data, we use the absolute value to highlight the differ-

ences. It is clear from Figure 13 that the quality of the solvent not only influences the equilibrium swelling (at $\epsilon = 0$) but also increases the rate of chain unravelling when compared to the $z = 0$ or (θ state) elongation. The curves in Figure 13 were obtained with $\tilde{h}^* = 0.19$ and $Wi = 2$. It was seen earlier that at $Wi = 2$ and $z = 1$ the stretch curves are not very sensitive to the choice of $\tilde{h}^*$ (Figure 8). Similar behavior was also observed for the other two solvent qualities displayed in Figure 13.

It is perhaps appropriate to conclude this section by reiterating that the parameter estimates $L = 22$ μm, $N_k = 200$, and $z = 1$, used to obtain theoretical predictions, are not adjustable parameters in the model but can be determined independently by experimental measurements. This combination has been shown to lead to a reasonable prediction of the experimental data of Smith and Chu. However, because of the uncertainty in the extent of blooming and the experimental error bars on $\bar{x}^+$, it is possible that other combinations of these parameters could also represent the data well.

7. Conclusion

A framework has been introduced for describing the behavior of dilute solutions of flexible macromolecules, which enables a consistent representation of the important physical phenomena of hydrodynamic interactions (HI), excluded-volume effects (EV), and finite extensibility. Incorporation of all these three nonlinear phenomena has been found to be essential in order to quantitatively explain the behavior of these solutions. The core problem of estimating the magnitude of parameters governing these effects has been addressed separately in the two regimes of behavior encountered in extensional flows, namely, (i) the universal regime where the chain is predominantly coiled and (ii) the nonuniversal regime where the chain unravels into a stretched state due to its finite size.

In the universal regime, two recently introduced methodologies for using Brownian dynamics simulations of bead−spring chain models with Hookean springs, namely, the procedure suggested by Kröger et al.[11] for examining the influence of hydrodynamic interactions in the nondraining limit and the procedure suggested by Kumar and Prakash[14] for obtaining the asymptotic behavior due to excluded-volume effects, have been combined to obtain parameter-free predictions in the presence of both HI and EV effects. In particular, the dependence of the expansion ratio E on the Hencky strain ϵ has been shown to become independent, in the long chain limit, of the hydrodynamic interaction parameter h^* and the range of excluded-volume interactions d^* (Figure 4). In this regime, the only variables required to describe the behavior of the solution are the radius of gyration under θ-conditions, R_g^θ, the solvent quality, z, and the Weissenberg number, Wi (Figure 5).

The modification of the definitions of the hydrodynamic interaction parameter, and the excluded-volume interactions parameter, as a consequence of using finitely extensible springs, has been examined by considering the approach of chains with finitely extensible springs to the long chain limit. While the rescaled HI parameter is $\tilde{h}^* = h^*/\chi$, the rescaled EV parameter is $\tilde{z}^* = (z^*/\chi^3)$, where χ is proportional to the nondimensional length of a single spring. As a result, though the predictions of universal ratios at equilibrium under θ-conditions are identical to those obtained with Hookean springs, universal behavior is attained in the nondraining limit $h = \tilde{h}^* \sqrt{N} \rightarrow \infty$ (Figure 1). Similarly, while the crossover dependence of the swelling of the polymer chain is identical to the prediction obtained with Hookean springs, the solvent quality parameter z is redefined as $z = \tilde{z}^*\sqrt{N}$ (Figure 2).

A description of finite size effects in elongational flow, for polymer chains with N_k Kuhn steps, has been obtained by introducing the successive fine-graining (SFG) procedure. In this two-step method, first, predictions of material properties are obtained with bead−spring chains consisting of progressively higher number of finitely extensible springs N, while keeping the contour length L, the radius of gyration R_g^θ, the solvent quality z, and the Weissenberg number Wi constant. In the second step, the accumulated data are extrapolated to the limit $(N - 1) \rightarrow N_k$. Though the results obtained with the SFG procedure are not strictly parameter-free, they were found to be relatively insensitive to the choice of $\tilde{h}^*$ in the range 0.19−0.30 (Figure 8) and to d^* (Figure 9) for $N_k = 200$. Interestingly, predictions of the expansion ratio for springs obeying two different force laws, namely, FENE and WLC, were found to differ from each other significantly only at large strain units (Figure 10). While the influence of excluded-volume effects is present at all values of strain in the case of infinite chains (Figure 5), EV effects die out as polymer molecules of finite length unravel to a stretched state (Figure 11).

Because of uncertainties in the persistence length of DNA and in the extent of video-camera blooming in the observations of stretch reported in ref 3, the values $R_g^\theta = 0.63$ μm (corresponding to $N_k = 200$) and $z = 1$ were used in this work in order to compare theoretical predictions with experimental results. Reasonable agreement between theory and experiment was found at both the Weissenberg numbers, $Wi = 2$ and $Wi = 55$, that were examined here (Figure 12).

The SFG procedure introduced here has opened up the exciting possibility of systematically studying the influence of HI, EV, and finite extensibility effects on the behavior of dilute polymer solutions far from equilibrium. This procedure, which enables an accurate modeling of the dynamics of DNA in high salt solutions with bead−spring chain models, could also prove to be a useful tool for computational biophysicists, since it is significantly less computationally expensive than using bead−rod chain models with bending potentials.[37]

Acknowledgment. This work has been supported by a grant from the Australian Research Council under the Discovery-Projects program. We thank Mr. R. Prabhakar for help with the development of the BDS codes and for very fruitful discussions. We are also grateful to Prof. Tam Sridhar for his suggestions and comments.

Appendix A. Rescaling of Interaction Parameters for FES at Equilibrium

The need to incorporate the finite extensibility of the spring arises only in flow situations where the Hookean (or linear) spring force model results in unphysical behavior of the predicted material functions of a dilute solution.[6] However, to be able to do so, it is essential to first understand the effects of finite extensibility at equilibrium. In this appendix, the influence of using finitely extensible springs on the scaling of equilibrium static and dynamic properties of a bead−spring chain model is analyzed using theoretical approximations and confirmed by the use of BDS.

The finite extensibility of the spring is incorporated by considering a model in which the spring force becomes singular at some finite extension. This introduces a parameter Q_0, which is the fully stretched length. Some of the commonly used spring force models are the finitely extensible nonlinear elastic (FENE) law, the inverse Langevin chain (ILC), and the wormlike chain (WLC). They may be represented in a general form consisting of a Hookean part and a nonlinear part $\mathbf{F}^c(\mathbf{Q}) = H\mathbf{Q}\,f(Q/Q_0)$, where the non-Hookean part $f(Q/Q_0)$ is given for the various cases by

$$f_{\mathrm{FENE}} = \frac{1}{1-q^2}$$

$$f_{\mathrm{ILC}} = \frac{3-q^2}{3(1-q^2)}$$

$$f_{\mathrm{WLC}} = \frac{1}{6q}\left(4q + \frac{1}{(1-q)^2} - 1\right) \tag{51}$$

where $q = Q/Q_0$. These expressions are statistical approximations to the equilibrium force extension behavior of a chain of discrete elements (segments or rods) and smoothly go from a linear regime at small extensions to singular behavior when fully stretched. The FENE and the ILC approximate a chain of freely jointed rods, and both these models have the same asymptotic behavior as $q \to 1$, the ILC being a Pade approximation to the actual inverse Langevin function.[10] The wormlike chain, however, has a distinctly different asymptotic behavior, and the above WLC expression[19] is a simple interpolation formula between the two limiting behaviors for the normalized extension as $q \to 0$ and $q \to 1$.

Considering a case when the only contribution to the potential energy of the chain comes from the spring force (i.e., a chain under θ-conditions) and using the force laws, it is straightforward to calculate equilibrium averages[6] of various moments of the distribution function ψ. In particular, we can find the covariance between two connector vectors to be $\langle \mathbf{Q}_\mu \mathbf{Q}_\nu \rangle = \langle Q^2 \rangle \delta_{\mu\nu}\boldsymbol{\delta}$, where $\langle Q^2 \rangle$ is the average evaluated using the equilibrium distribution for a single spring. In three dimensions this can be written in a general form as

$$\langle Q^2 \rangle = 3\chi^2(b)\frac{kT}{H} \tag{52}$$

Here we introduce the function $\chi(b)$ which can be evaluated with the knowledge of the force law for the finitely extensible spring. For a FENE spring this can be written explicitly as[6]

$$\chi^2(b) = \frac{b}{b+5} \quad \text{(for FENE)} \tag{53}$$

In the asymptotic limit of $b \to \infty$, which corresponds to a linear spring force by construction of the nonlinear part f, we recover the Hookean result for $\langle Q^2 \rangle$, in which case, $\chi(b) \to 1$. The function $\chi(b)$ is therefore bounded between zero and unity.

We now obtain some general exact results for a chain of connected springs in equilibrium. The static properties can be written down explicitly under θ-conditions. The end-to-end vector for the chain is $\mathbf{R}_e = \sum_\mu^{N-1}\mathbf{Q}_\mu$, and the average mean-square end-to-end distance is $\langle R_e^2 \rangle = (N-1)\langle Q^2 \rangle$. As a result, using eq 52, we obtain at equilibrium

$$\langle R_e^2 \rangle = 3(N-1)\chi^2(b)\frac{kT}{H} \tag{54}$$

It can be shown that the mean-square gyration radius with an arbitrary spring force law at equilibrium is[6]

$$\langle R_g^2 \rangle = \langle R_e^2 \rangle \frac{N+1}{6N} \tag{55}$$

$$\langle R_g^2 \rangle = \chi^2(b)\frac{N^2-1}{2N}\frac{kT}{H} \tag{56}$$

These results for the static properties are exact in N and are applicable for any spring force law under θ-conditions. While similar closed form expressions cannot be obtained under good-solvent conditions and for dynamic properties even under θ-conditions, they can be obtained by a numerical method (such as BDS), as will be discussed later in this section. Nevertheless, the asymptotic behavior of these properties can be obtained by some analytical approximations, which are given for each of the cases below.

A.1. Rescaling of the HI Parameter. In the presence of HI between the beads, as discussed in section 2, the HI tensor is often approximated using the Oseen tensor given in eq 7. It is known that this approximation has a limitation for small values of $r_{\mu\nu}$ and requires a correction.[22] However, this correction can be ignored in the long chain limit of $N \to \infty$, for an analytical treatment. In the equilibrium averaged approximation, the tensor, which is a function of the bead positions, is replaced by an isotropic constant tensor $\boldsymbol{\Omega}_{\mu\nu} \to \langle \boldsymbol{\Omega}_{\mu\nu} \rangle_{\mathrm{eq}}$, which is given by[6]

$$\langle \boldsymbol{\Omega}_{\mu\nu} \rangle_{\mathrm{eq}} = \frac{1-\delta_{\mu\nu}}{6\pi\eta_s}\left\langle \frac{1}{r_{\mu\nu}} \right\rangle_{\mathrm{eq}} \boldsymbol{\delta} \tag{57}$$

The ensemble average appearing in the above equation can be carried out using the equilibrium distribution function of the vector between any two bead positions $\mathbf{r}_{\mu\nu}$. For a bead−spring chain with Hookean springs, in which the distribution function for the vector between adjacent beads is Gaussian by definition, it can be shown that the probability density $P(\mathbf{r}_{\mu\nu})$ for any two beads is also a Gaussian[6] and is given by

$$P(\mathbf{r}_{\mu\nu}) = \left(\frac{1}{2\pi\sigma_H^2}\right)^{3/2} e^{-r_{\mu\nu}^2/2\sigma_H^2} \tag{58}$$

where $\sigma_H^2 = |\mu-\nu|(kT/H)$. It is then straightforward to evaluate

$$\left\langle \frac{1}{r_{\mu\nu}} \right\rangle_{\mathrm{eq}} = \sqrt{\frac{2}{\pi\sigma_H^2}} = \sqrt{\frac{2H}{\pi kT}}\sqrt{\frac{1}{|\mu-\nu|}} \tag{59}$$

In the case of a finitely extensible spring the distribution function between adjacent beads is not Gaussian, and therefore the probability density $P(\mathbf{r}_{\mu\nu})$ cannot be reduced to a Gaussian, as in the case of Hookean springs above. However, we can make an approximation when $|\mu-\nu| \gg 1$. Since adjacent springs are "freely jointed" (independent) at the bead center, we know from the central limit theorem that the distribution function for the vector $\mathbf{r}_{\mu\nu}$ will be Gaussian for $|\mu-\nu| \gg 1$ and will be given by

$$P(\mathbf{r}_{\mu\nu}) \approx \left(\frac{1}{2\pi\sigma_F{}^2}\right)^{3/2} e^{-r_{\mu\nu}{}^2/2\sigma_F{}^2} \tag{60}$$

where $\sigma_F{}^2 = |\mu - \nu|\ell^2$ and ℓ is the characteristic length of a spring. For an arbitrary force law this is given by $\ell^2 = \langle Q^2\rangle/3$ and along with eq 52 we can write for any force law

$$\sigma_F{}^2 = |\mu - \nu|\chi^2(kT/H) \tag{61}$$

The average occurring in the hydrodynamic interaction tensor can then be written as

$$\left\langle \frac{1}{r_{\mu\nu}} \right\rangle_{eq} =$$

$$\begin{cases} \sqrt{\dfrac{2}{\pi\sigma_F{}^2}} = \sqrt{\dfrac{2}{\pi}}\dfrac{1}{l_H}\dfrac{1}{\chi}\sqrt{\dfrac{1}{|\mu-\nu|}}, & \text{for } |\mu-\nu| > |\mu-\nu|_{min} \\ \sqrt{\dfrac{2}{\pi}}\dfrac{1}{l_H}\dfrac{1}{\chi}\sqrt{\dfrac{1}{|\mu-\nu|}}(1+f(\chi,|\mu-\nu|)) & \text{otherwise} \end{cases} \tag{62}$$

The first case in the above expression represents the situation where the average is evaluated with a Gaussian distribution, corresponding to beads for which $|\mu - \nu| > |\mu - \nu|_{min}$. In the second case, the function $f(\chi, |\mu - \nu|)$ represents the value of the analytically unknown average that arises due to the distribution function $P(\mathbf{r}_{\mu\nu})$ being non-Gaussian for beads with $|\mu - \nu| < |\mu - \nu|_{min}$. An estimate of the bounds on $|\mu - \nu|_{min}$ can be provided by the following argument. For a freely jointed bead−rod chain, $|\mu - \nu|_{min} \approx 10$ leads to a Gaussian distribution for the end-to-end vector. On the other hand, we know from eq 58 that for a chain of Hookean springs even the vector between adjacent beads obeys a Gaussian distribution, implying $|\mu - \nu|_{min} = 1$. Therefore, we can anticipate that for a finitely extensible spring, with a stiffness parameter b varying from infinity (Hookean) to zero (rodlike), that $1 < |\mu - \nu|_{min} \lesssim 10$. The function $f(\chi, |\mu - \nu|)$ must also clearly satisfy the requirement that $f(\chi, |\mu - \nu|) \to 0$, as $\chi \to 1$.

We now obtain the scaling of the diffusivity for a chain of finitely extensible springs and make some generalizations based on this. The translational diffusion coefficient under θ-conditions in the preaveraged approximation is given by[6]

$$\bar{\mathscr{D}}^\theta = \frac{kT}{N\zeta}\left(1 + \frac{h^*\sqrt{\pi}}{N}\sqrt{\frac{kT}{H}}\sum_{\substack{\mu,\nu \\ \mu\neq\nu}}\left\langle\frac{1}{r_{\mu\nu}}\right\rangle_{eq}\right) \tag{63}$$

Substituting eq 62, converting sums to integrals, and taking into account the correction due to the singularity at $\mu = \nu$,[29,38] we obtain in the limit $N \gg 1$

$$\bar{\mathscr{D}}^\theta = \frac{kT}{N\zeta}\left[1 + \frac{h^*}{\chi}\left(\frac{8}{3}\sqrt{2N} - \frac{1}{h^*_{Zf}}\right)\right] + \mathscr{O}(N^{-3/2}) + \frac{kT}{N\zeta}\frac{\sqrt{2}h^*}{N\chi}g(\chi,N) \tag{64}$$

where $g(\chi,N) = \sum_{\mu,\nu;|\mu-\nu|<|\mu-\nu|_{min}} f(\chi, |\mu - \nu|)/\sqrt{|\mu-\nu|}$ represents non-Gaussian contributions to the sum in eq 63, and $h^*_{Zf} \approx 12/35\sqrt{2} = 0.2424$. (A further small refinement to this calculation can be obtained,[39] which gives $h^*_{Zf} = 0.242\,16$.) The only difference between the Zimm result (for Hookean springs) and eq 64 is the presence of the functions χ and $g(\chi,N)$. It is instructive to examine the behavior of universal ratios at this juncture. The ratio of radius of gyration and the hydrodynamic radius can be written as

$$U_{R\bar{D}} \equiv \frac{R_g}{R_H} \equiv \frac{6\pi\eta_s}{kT}\bar{\mathscr{D}}^\theta R_g = \frac{1}{\sqrt{\pi}h^*}R_g\sqrt{\frac{H}{kT}}\frac{\bar{\mathscr{D}}^\theta\zeta}{kT} \tag{65}$$

In the limit of large N we can write eq 56 as $R_g = \chi\sqrt{N/2}\sqrt{kT/H}$, and with eq 64 we have

$$U_{R\bar{D}} = \frac{8}{3\sqrt{\pi}} + \frac{1}{\sqrt{2\pi N}}\left(\frac{\chi}{h^*} - \frac{1}{h^*_{Zf}}\right) + \mathscr{O}(N^{-1}) + \frac{1}{\sqrt{\pi}N^{3/2}}g(\chi,N) \tag{66}$$

Since the long chain limit must remain unchanged regardless of the force law used to describe the springs, we can write the expansion

$$g(\chi,N) = g_0(\chi)N + g_1(\chi)\sqrt{N} + \ldots \tag{67}$$

This implies that, correct to leading order, the universal ratio can be written as

$$U_{R\bar{D}} = \frac{8}{3\sqrt{\pi}} + \frac{1}{\sqrt{2\pi N}}\left(\frac{\chi}{h^*} - \frac{1}{h^*_f(\chi)}\right) + \mathscr{O}(N^{-1}) \tag{68}$$

where

$$\frac{1}{h^*_f(\chi)} = \frac{1}{h^*_{Zf}} - \sqrt{2}g_0(\chi) \tag{69}$$

Comparing eq 68 with the Zimm expression for Hookean springs

$$U_{R\bar{D}} = \frac{8}{3\sqrt{\pi}} + \frac{1}{\sqrt{2\pi N}}\left(\frac{1}{h^*} - \frac{1}{h^*_{Zf}}\right) + \mathscr{O}(N^{-1}) \tag{70}$$

it can be concluded that (i) in the presence of finitely extensible springs a rescaled hydrodynamic interaction parameter can be defined by absorbing the factor $1/\chi$ into the definition of h^*

$$\tilde{h}^* = \frac{h^*}{\chi(b)} \tag{71}$$

and (ii) the fixed point is modified and becomes a function of χ, as can be seen from eq 69. In general, any universal ratio in the presence of finitely extensible springs can consequently be written in the form

$$U_\phi = U^\infty_\phi + c_\phi\left(\frac{1}{\tilde{h}^*} - \frac{1}{h^*_f(\chi)}\right)\frac{1}{\sqrt{N}} + \mathscr{O}\left(\frac{1}{N}\right) \tag{72}$$

A close parallel can be drawn with the results obtained for a chain with consistently averaged HI and finite extensibility.[26] In this approximation the equilibrium distribution function is replaced by a Gaussian distribution as in the FENE-P model. In such an approximation for FENE springs, one obtains $\chi^2(b) = b/(b+3)$, instead of eq 53, and the whole treatment can

be carried out with the rescaled interaction parameter $\tilde{h}^*$ in eq 71, as was shown in ref 26.

A.2. Rescaling of EV Interactions. In this work, excluded-volume effects have been incorporated in a bead−spring chain model by using a narrow-Gaussian potential, given in eq 4. Kumar and Prakash[14] have recently established that, in the long chain limit, this potential correctly captures both the solvent quality crossover and the excluded-volume limit behavior of Hookean chains. It was shown that in this limit the only relevant parameter is the solvent quality z, expressed in terms of the model variables as $z = z^*\sqrt{N}$. However, this interpretation of solvent quality in terms of the model variables cannot be directly carried over to the case of a chain of finitely extensible springs, and a reinterpretation of z in terms of model parameters is necessary.

As pointed out earlier, it is difficult to obtain exact expressions for the static properties with excluded-volume interactions. However, a perturbation expansion in the strength of interactions can be carried out.[5,13] Here we present some essential steps required to obtain the perturbation parameter when carrying out an expansion in small excluded-volume effects using the narrow-Gaussian potential. The derivation is based on an expansion obtained for a chain of Hookean springs,[40] which we extend to the case of finitely extensible springs. The easiest starting point is the calculation of the swelling of a static property, such as the root-mean-square end-to-end distance

$$\langle R_e^2\rangle = \sum_{i,j}^{N-1}\langle \mathbf{Q}_i\cdot\mathbf{Q}_j\rangle, \tag{73}$$

which requires the evaluation of the covariance at equilibrium

$$\langle \mathbf{Q}_i\mathbf{Q}_j\rangle = \frac{1}{\mathcal{N}}\int d\mathbf{Q}^{N-1}\, e^{-\phi/kT}\mathbf{Q}_i\mathbf{Q}_j \tag{74}$$

where the normalizing constant

$$\mathcal{N} = \int d\mathbf{Q}^{N-1}\, e^{-\phi/kT} \tag{75}$$

and ϕ is the potential energy of the chain given by

$$\phi = \sum_{k=1}^{N-1}\phi_k^s + \frac{1}{2}\sum_{\substack{\mu,\nu=1\\ \mu\neq\nu}}^{N}\phi^e(\mathbf{r}_{\mu\nu}) \tag{76}$$

where ϕ_k^s is the entropic spring potential for a spring k, obtained from the nonlinear model for the force chosen, and ϕ^e is the narrow-Gaussian potential in eq 4. In the following, we omit explicit limits on sums for ease of notation, and the limits given above should be taken appropriately. The weighting function in the moment equation (eq 74) can be expanded to first order in EV effects

$$e^{-\phi/kT} = \prod_k e^{-\phi_k^s/kT}\left[1 - \frac{1}{2kT}\sum_{\mu\neq\nu}\phi^e(\mathbf{r}_{\mu\nu})\right] \tag{77}$$

Before we evaluate the covariance, we need to find the normalization constant correct to first order. It can be shown that

$$\mathcal{N} = \mathcal{N}_\theta\left[1 - \frac{1}{2kT}\sum_{\mu\neq\nu}\langle\phi^e(\mathbf{r}_{\mu\nu})\rangle_\theta\right] \tag{78}$$

where

$$\mathcal{N}_\theta = \prod_k\int d\mathbf{Q}^{N-1}\, e^{-\phi_k^s/kT} \tag{79}$$

for the leading order potential, and $\langle\phi^e\rangle_\theta$ is the ensemble average evaluated with the distribution at θ-conditions

$$\langle\phi^e\rangle_\theta = \frac{1}{\mathcal{N}_\theta}\prod_k\int d\mathbf{Q}^{N-1}\, e^{-\phi_k^s/kT}(\phi^e) \tag{80}$$

To evaluate $\langle\phi^e\rangle_\theta$, we recognize that, similar to the case of HI, EV is a "long-range" effect; i.e., the interactions are between parts of the chain that are far separated along the chain length are responsible for the macroscopic properties.[5] Therefore, we can make the same approximation as we did before and use eq 60 (which is a Gaussian distribution) to evaluate the equilibrium average $\langle\phi^e\rangle_\theta$. Since ϕ^e is also a Gaussian, we can show

$$\langle\phi^e(\mathbf{r}_{\mu\nu})\rangle_\theta = \frac{vkT}{(2\pi\sigma_z^2)^{3/2}} \tag{81}$$

where $\sigma_z^2 = d^2 + \sigma_F^2$. Substituting this in eq 78 and expanding $1/\mathcal{N}$ to first order in v, which is required for evaluating the moments, we have

$$\frac{1}{\mathcal{N}} = \frac{1}{\mathcal{N}_\theta}\left[1 + \sum_{\mu\neq\nu}\frac{v}{2(2\pi\sigma_z^2)^{3/2}}\right] \equiv \frac{1}{\mathcal{N}_\theta}\left(1 + \frac{1}{\tilde{\mathcal{N}}}\right) \tag{82}$$

which also defines $\tilde{\mathcal{N}}$. We now find $\langle\mathbf{Q}_i\mathbf{Q}_j\rangle$, correct to first order in v, to be

$$\langle\mathbf{Q}_i\mathbf{Q}_j\rangle = \frac{\mathcal{N}_\theta}{\mathcal{N}}\langle\mathbf{Q}_i\mathbf{Q}_j\rangle_\theta - \frac{1}{2kT}\frac{\mathcal{N}_\theta}{\mathcal{N}}\sum_{\mu\neq\nu}\langle\mathbf{Q}_i\mathbf{Q}_j\,\phi^e(\mathbf{r}_{\mu\nu})\rangle_\theta \tag{83}$$

$$\langle\mathbf{Q}_i\mathbf{Q}_j\rangle = \langle\mathbf{Q}_i\mathbf{Q}_j\rangle_\theta\left(1 + \frac{1}{\tilde{\mathcal{N}}}\right) - \frac{1}{2kT}\sum_{\mu\neq\nu}\langle\mathbf{Q}_i\mathbf{Q}_j\phi^e(\mathbf{r}_{\mu\nu})\rangle_\theta \tag{84}$$

Therefore, to evaluate the second moment to first order, we only have to evaluate averages with Gaussian distributions, a convenience brought about due to the assumption of a narrow-Gaussian potential for EV effects. Following the approach given in ref 41 to decompose complex moments of Gaussian distribution for a multidimensional Gaussian distribution in several variables, we can show that

$$\langle\mathbf{Q}_i\mathbf{Q}_j\phi^e(\mathbf{r}_{\mu\nu})\rangle_\theta = \langle\phi^e(\mathbf{r}_{\mu\nu})\rangle_\theta \times \left[\langle\mathbf{Q}_i\mathbf{Q}_j\rangle_\theta - \frac{1}{\sigma_z^2}\langle\mathbf{Q}_i\mathbf{Q}_j\phi^e(\mathbf{r}_{\mu\nu})\rangle_\theta\cdot\langle\mathbf{r}_{\mu\nu}\mathbf{Q}_j\rangle_\theta\right] \tag{85}$$

Finally, it follows from eq 84 that

$$\langle\mathbf{Q}_i\mathbf{Q}_j\rangle = \langle\mathbf{Q}_i\mathbf{Q}_j\rangle_\theta + \sum_{\mu\neq\nu}\frac{v}{2(2\pi\sigma_z^2)^{3/2}}\frac{1}{\sigma_z^2}\langle\mathbf{Q}_i\mathbf{r}_{\mu\nu}\rangle_\theta\cdot\langle\mathbf{r}_{\mu\nu}\mathbf{Q}_j\rangle_\theta \tag{86}$$

Using the following identities, which are again simple Gaussian averages

$$\langle \mathbf{Q}_i \mathbf{Q}_j \rangle_\theta = \chi^2 \frac{kT}{H} \boldsymbol{\delta} \delta_{ij} \tag{87}$$

$$\langle \mathbf{Q}_i \mathbf{r}_{\mu\nu} \rangle_\theta = \chi^2 \frac{kT}{H} \boldsymbol{\delta} \sum_{k=\mu}^{\nu-1} \delta_{ik} \quad \text{for } \mu < \nu \tag{88}$$

and observing that $\mathbf{r}_{\mu\nu}$ occurs as an even multiple, implying the indices μ and ν can be swapped to obey $\mu < \nu$, we can show that

$$\langle \mathbf{Q}_i \mathbf{Q}_j \rangle = \chi^2 \frac{kT}{H} \boldsymbol{\delta} \times \left[\delta_{ij} + \sum_{\mu \neq \nu} \frac{1}{2} \frac{v}{(2\pi {\sigma_z}^2)^{3/2}} \chi^2 \frac{kT}{H} \frac{1}{{\sigma_z}^2} \sum_{k,l=\mu}^{\nu-1} \delta_{ik} \delta_{jl} \right] \tag{89}$$

With the following identities and simplifications (using eq 61)

$${\sigma_z}^2 = \chi^2 \frac{kT}{H} \sigma_z^{*2} \tag{90}$$

$$\sigma_z^{*2} \equiv \left[\frac{d^{*2}}{\chi^2} + |\mu - \nu| \right] \tag{91}$$

$$\frac{v}{(2\pi {\sigma_z}^2)^{3/2}} = \frac{z^*}{(\chi^2 \sigma_z^{*2})^{3/2}} \tag{92}$$

$$z^* \equiv \frac{v}{(2\pi kT/H)^{3/2}} \tag{93}$$

we can write the final expression for the covariance from eq 89 as

$$\langle \mathbf{Q}_i \mathbf{Q}_j \rangle = \chi^2 \frac{kT}{H} \boldsymbol{\delta} \left[\delta_{ij} + \frac{z^*}{2\chi^3} \sum_{\mu \neq \nu} \frac{1}{\sigma_z^{*5}} \theta(\mu,i,j,\nu) \right] \tag{94}$$

where we have used the convenient notation introduced in ref 41

$$\theta(\mu,i,j,\nu) = \begin{cases} 1 & \text{if } (\mu \leq i, j < \nu) \text{ or } (\nu \leq i, j < \mu) \\ 0 & \text{otherwise} \end{cases} \tag{95}$$

which picks only those μ, ν that span a range across i and j. Substituting the expression for the covariance in eq 73, converting the sums to integrals in the limit $N \rightarrow \infty$, as given in ref 40, the actual perturbation parameter for excluded-volume effects can be shown to be equal to

$$z = \frac{z^*}{\chi^3} \sqrt{N} \tag{96}$$

This provides the definition of the solvent quality in terms of the model parameters. With this redefinition, the swelling ratio of the radius of gyration can be obtained using a chain of finitely extensible springs. Just as the universal ratios do not depend on the force law, we expect the crossover functions to be universal functions of z and consequently the same irrespective of the nature of the springs used to obtain the crossover. Using BDS, we have demonstrated that this is indeed the case.

A.3. Physical Interpretation of Rescaling. While the discussion of the rescaling of HI and EV interaction parameters above has been carried out on formal grounds, it is instructive to provide a physical interpretation of the rescaling. First, to understand the meaning of χ, we turn to eq 52: for a Hookean force law, where $\chi = 1$, we can interpret $\sqrt{kT/H}$ to be the characteristic length of a single spring. In standard treatments,[18] this has been considered as the characteristic length $l_H \equiv \sqrt{kT/H}$ used to nondimensionalize the governing equations. For any finitely extensible spring, it is clear from eq 52 that χ is the characteristic length of the spring in the units of $\sqrt{kT/H}$. The HI parameter h^*, which has been considered to represent a nondimensional effective hydrodynamic radius, eq 13, for the Hookean springs, must be reinterpreted in a more general way as the ratio of the bead radius to the characteristic length of the spring, so that the important nondimensional number characterizing the strength of HI should be

$$\tilde{h}^* = \frac{\text{bead radius}}{\text{characteristic length of a spring}} \tag{97}$$

$$\tilde{h}^* = \frac{1}{\sqrt{\pi}} \frac{a}{\chi \sqrt{kT/H}} = \frac{h^*}{\chi} \tag{98}$$

as has appeared naturally in eq 68.

Similarly, in the case of EV, the local parameter is a volume term v and the important nondimensional parameter characterizing excluded-volume interactions can be written down from eq 93 as

$$\tilde{z}^* = \frac{\text{excluded volume}}{\text{cube of the characteristic length of a spring}} \tag{99}$$

$$\tilde{z}^* = \frac{1}{(2\pi)^{3/2}} \frac{v}{(\chi \sqrt{kT/H})^3} = \frac{z^*}{\chi^3} \tag{100}$$

This reinterpretation of HI and EV parameters is consistent with Hookean results with $\chi = 1$.

Appendix B. Evaluation of $\chi(b)$ for a WLC

The factor $\chi(b)$ is defined by the nondimensional second moment in eq 52. The distribution function with which the moment is evaluated is simply that of the connector vector of a single spring (or a dumbbell)

$$\psi_{\text{eq}}(\mathbf{Q}) = \frac{\mathrm{e}^{-\phi/kT}}{\int \mathrm{d}\mathbf{Q}\, \mathrm{e}^{-\phi/kT}} \tag{101}$$

with ϕ given by $\mathbf{F}^c = \partial\phi/\partial\mathbf{Q}$. Nondimensionalizing length by $\sqrt{kT/H}$, inserting the WLC force model expression from eqs 51, and performing the integration in spherical coordinates, the expression for χ can be written as

$$\chi^2(b) = \frac{1}{3} \frac{\int_0^1 \mathrm{d}q\, q^4 \mathrm{e}^{-\phi^*}}{\int_0^1 \mathrm{d}q\, q^2 \mathrm{e}^{-\phi^*}} \tag{102}$$

where $\phi^* = (b/6)[2q^2 + 1/(1-q) - q]$. This integral is not known in closed form; however, it might be evaluated by using a numerical quadrature. We present some

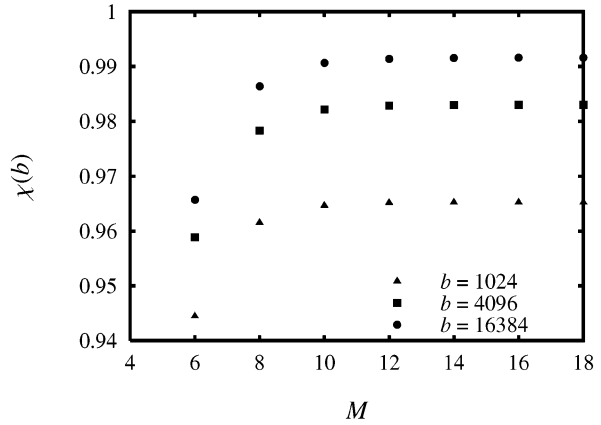

Figure 14. Approach of χ to its asymptotic value, for various values of b.

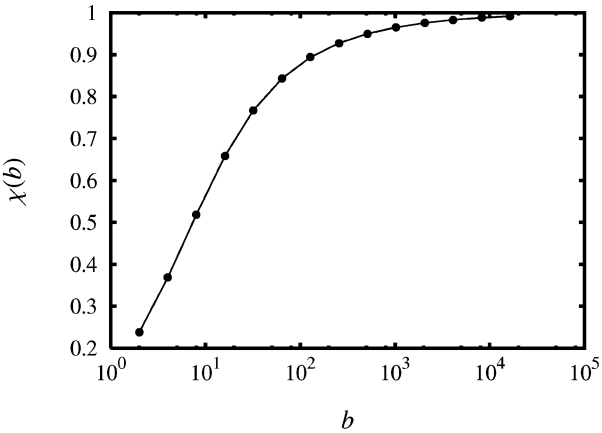

Figure 15. Dependence of the characteristic nondimensional length, χ, of a wormlike spring on the parameter b.

useful approximations to evaluate this integral numerically. Consider the integral in general

$$I_n(b) = \int_0^1 \mathrm{d}q\; q^n \mathrm{e}^{-(b/6)(2q^2+1/(1-q)-q)} \qquad (103)$$

where n is any number. The problem of evaluating this integral numerically using a generic formula arises because, for very large b, the contributions beyond a certain value of q become negligible, and to obtain an accurate value of the integral, several quadrature points need to be placed in the whole interval $0 < q < 1$, so that the dominant interval is well represented. To overcome this problem, we perform a rescaling of the integral and obtain its value in an asymptotic limit. This is done by evaluating the integral only up to a certain value of q. The upper bound of this integration is found in the following manner. We first note that for large b contributions come from $q \ll 1$, in which limit we can approximate $\phi^* \approx b/6 + bq^2/2$. Therefore, we have for large b

$$I_n(b) \approx \mathrm{e}^{-b/6} \int_0^1 \mathrm{d}q\; q^n \mathrm{e}^{-bq^2/2} \qquad (104)$$

The contributions to this integral for $q > \sqrt{2M/b}$ can be neglected, where M is a large number. This provides an upper bound so that we can write eq 103 as

$$I_n(b) = \lim_{M \to b/2} \int_0^{\sqrt{2M/b}} \mathrm{d}q\; q^n \mathrm{e}^{-\phi^*} \qquad (105)$$

With this rescaling, the integral can be evaluated with a small number of Gauss quadrature points: what has been essentially achieved is that the quadrature points are efficiently spaced in the dominant interval.

The evaluation of the integral with the WLC force model has an additional complication. This arises from the small q behavior of ϕ^* where $\phi^* \sim b/6 + bq^2/2$. Note that there is an additional constant apart from the Hookean factor. Though this does not have any consequence for the physics of the problem, since in the force expression (used in the BDS) this term is zero upon differentiation, it does lead to numerical problems in evaluation of the integral for large b. For large b this leads to (a) floating point overflow, in both the numerator and the denominator in eq 102 because of the presence of the constant $\mathrm{e}^{-b/6}$ as well as (b) a precision error when one small number is divided by another. To overcome this, we multiply the numerator and denominator of eq 102 by $\mathrm{e}^{b/6}$, which will not alter the integral and which also leads to the correct Hookean limit for $q \ll 1$.

Using these approximations, χ can be evaluated for a given value of b. The behavior of χ as a function of M for various values of b is shown in Figure 14. The value of χ approaches its asymptotic value to within four digits of accuracy even for $M = 18$. The function $\chi(b)$ so obtained is shown in Figure 15. We note that this procedure can be uniformly applied to any value of b and is also common to all finitely extensible force laws where no closed form solutions are available for $\chi(b)$.

Note Added after ASAP Publication. The correct reference 4 was inadvertantly omitted from the version posted ASAP December 15, 2004; the corrected version was posted December 29, 2004.

References and Notes

(1) Perkins, T. T.; Quake, S. R.; Smith, D. E.; Chu, S. *Science* **1994**, *264,* 822−826.
(2) Smith, D. E.; Perkins, T. T.; Chu, S. *Macromolecules* **1996**, *29,* 1372−1373.
(3) Smith, D. E.; Chu, S. *Science* **1998**, *281,* 1335−1340.
(4) Schroeder, C. M.; Babcock, H. P.; Shaqfeh, E. S. G.; Chu, S. *Science* **2003**, *301*, 1515.
(5) Doi, M.; Edwards, S. F. *The Theory of Polymer Dynamics;* Clarendon Press: Oxford, 1986.
(6) Bird, R. B.; Curtiss, C. F.; Armstrong, R. C.; Hassager, O. *Dynamics of Polymeric Liquids*, 2nd ed.; John Wiley: New York, 1987; Vol. 2.
(7) Larson, R. G.; Hu, H.; Smith, D. E.; Chu, S. *J. Rheol.* **1999**, *43,* 267−304.
(8) Jendrejack, R. M.; de Pablo, J. J.; Graham, M. D. *J. Chem. Phys.* **2002**, *116,* 7752−7759.
(9) Hsieh, C.-C.; Li, L.; Larson, R. G. *J. Non-Newtonian Fluid Mech.* **2003**, *113,* 147−191.
(10) Yamakawa, H. *Modern Theory of Polymer Solutions;* Harper and Row: New York, 1971.
(11) Kröger, M.; Alba-Pérez, A.; Laso, M.; Öttinger, H. C. *J. Chem. Phys.* **2000**, *113,* 4767−4773.
(12) Miyaki, Y.; Fujita, H. *Macromolecules* **1981**, *14,* 742−746.
(13) Schäfer, L. *Excluded Volume Effects in Polymer Solutions;* Springer-Verlag: Berlin, 1999.
(14) Kumar, K. S.; Prakash, J. R. *Macromolecules* **2003**, *36,* 7842−7856.
(15) Prakash, J. R.; Öttinger, H. C. *J. Non-Newtonian Fluid Mech.* **1997**, *71,* 245−272.
(16) Prakash, J. R. *J. Rheol.* **2002**, *46,* 1353−1380.
(17) Kumar, K. S.; Prakash, J. R. *J. Chem. Phys.* **2004**, *121,* 3886−3897.
(18) Öttinger, H. C. *Stochastic Processes in Polymeric Fluids;* Springer: Berlin, 1996.
(19) Marko, J. F.; Siggia, E. D. *Macromolecules* **1995**, *28,* 8759−8770.
(20) Prakash, J. R.; Öttinger, H. C. *Macromolecules* **1999**, *32,* 2028−2043.

(21) Prakash, J. R. *Macromolecules* **2001**, *34,* 3396−3411.
(22) Rotne, J.; Prager, S. *J. Chem. Phys.* **1969**, *50,* 4831−4837.
(23) Jendrejack, R. M.; Graham, M. D.; de Pablo, J. J. *J. Chem. Phys.* **2000**, *113,* 2894−2900.
(24) Fixman, M. *Macromolecules* **1986**, *19,* 1204−1207.
(25) Prabhakar, R.; Prakash, J. R. *J. Non-Newtonian Fluid Mech.* **2004**, *116,* 163−182.
(26) Öttinger, H. C. *J. Non-Newtonian Fluid Mech.* **1987**, *26,* 207−246.
(27) Miyaki, Y.; Einaga, Y.; Fujita, H.; Fukuda, M. *Macromolecules* **1980**, *13,* 588−592.
(28) Zimm, B. H. *J. Chem. Phys.* **1956**, *24,* 269−281.
(29) Osaki, K. *Macromolecules* **1972**, *5,* 141−144.
(30) de Gennes, P.-G. *Scaling Concepts in Polymer Physics*; Cornell University Press: Ithaca, NY, 1979.
(31) Prabhakar, R.; Prakash, J. R.; Sridhar, T. *J. Rheol.* **2004**, *48*, 1251−1278.
(32) Louis Barrat, J.; Joanny, J.-F. *Adv. Chem. Phys.* **1996**, *94,* 1−66.
(33) Perkins, T. T.; Smith, D. E.; Chu, S. *Science* **1997**, *276,* 2016−2021.
(34) Bustamante, C.; Marko, J. F.; Siggia, E. D.; Smith, S. *Science* **1994**, *265,* 1599−1600.
(35) Quake, S. R.; Babcock, H.; Chu, S. *Nature (London)* **1997**, *388,* 151−154.
(36) Eisenberg, H. *Acta Polym.* **1998**, *49,* 534−538.
(37) Klenin, K.; Merlitz, H.; Langowski, J. *Biophys. J.* **1998**, *74,* 780−788.
(38) Öttinger, H. C. *J. Chem. Phys.* **1987**, *86,* 3731−3749.
(39) Sunthar, P. Unpublished notes, 2003.
(40) Prakash, J. R. *Chem. Eng. Sci.* **2001**, *56,* 5555−5564.
(41) Öttinger, H. C. *J. Chem. Phys.* **1989**, *90,* 463−473.

MA035941L